BADLANDS

9

Alan D. Howard

BADLAND REGOLITH AND PROCESSES

Badlands have fascinated geomorphologists for the same reasons that they inhibit agricultural use: lack of vegetation, steep slopes, high drainage density, shallow to non-existent regolith, and rapid erosion rates. Badlands appear to offer in a miniature spatial scale and a shortened temporal scale many of the processes and landforms exhibited by more normal fluvial landscapes, including a variety of slope forms, bedrock or alluvium-floored rills and washes, and flat alluvial expanses similar to large-scale pediments. The often (but not universally) rapid landform evolution provides the prospect of direct observational coupling of process and landform evolution in both natural and man-induced badlands. However, Campbell (1989) and Campbell and Honsaker (1982) caution about problems of scaling between processes on badland slopes and channels to larger landforms. Furthermore, although badland slopes are commonly quite regular in appearance (Fig. 9.1), recent studies have demonstrated that weathering, mass wasting, and water erosional processes on badland slopes exhibit complex spatial and temporal variability, and that the weathering and erosional processes are largely hidden from direct observation in cracks and micropipes (Bryan *et al.* 1978, Yair *et al.* 1980).

This chapter will emphasize the relationship between process and form in badland landscapes and the long-term evolution of badland landscapes through both descriptive and quantitative modelling. More general reviews of badlands and badland processes are provided by Campbell (1989) and Bryan and Yair (1982a), including discussion of the climatic, geologic, and geographic setting of badlands, sediment yields, host rock and regolith variations among badlands, field measurements of processes, and badland gullies and piping.

AN EXAMPLE: BADLANDS IN THE HENRY MOUNTAINS AREA, UTAH

Shales of Jurassic and Cretaceous age exposed in the vicinity of the Henry Mountains, Utah, have in places been sculpted into dramatic badlands. The climate in the desert areas at about 1500 m above mean sea level is arid, with about 125 mm of annual precipitation, most of which occurs as summer thunderstorms. These badlands provide premier examples of the erosional conditions favouring badlands, badland slope form and process, relationship between fluvial and slope processes, and variations of badland form with rock type. In particular, the great thickness and uniform lithology of the Upper Cretaceous Mancos Shale (Hunt 1953) results in an unusual regularity of slope form and process (Fig. 9.1), first described by Gilbert (1880). Badlands developed in this area on the Mancos Shale, the Morrison Formation, and the Summerville Formation will be used here as examples. These badlands are discussed more fully by Howard (1970).

BADLAND REGOLITH

Badlands generally have very thin regoliths in arid regions, ranging from about 30 cm to essentially unweathered bedrock. Many badland areas share a similar regolith profile. The top 1 to 5 cm is a surface layer exhibiting desiccation cracks when dry. This surface layer is compact with narrow polygonal cracking in the case of shales with modest shrink–swell (<25%) behaviour, such as the Mancos Shale badlands in Utah (Fig. 9.1), the Brule Formation badlands in South Dakota (Schumm 1956a, b), and portions of the Dinosaur Badlands, Canada (Bryan *et al.* 1978, 1984, Hodges and Bryan 1982). With higher shrink–swell behaviour the surface layer is broken into irregular, loose 'popcorn' fragments with large intervening voids, as exemplified in badlands on the

Geomorphology of Desert Environments. Edited by Athol D. Abrahams and Anthony J. Parsons. Published in 1994 by Chapman & Hall, London. ISBN 0 412 44480 1.

Figure 9.1 Badlands in Mancos Shale, near the Henry Mountains, Utah. Note linearity of slope profile and narrowness of divides.

Chadron Formation in South Dakota, the Morrison (Fig. 9.2) and Chinle Formations in Utah, and portions of the Dinosaur Badlands, Canada. The surface layer may be thicker (≥10 cm) in such cases. Although the surface layer may contain a few partially weathered fragments of shale, vein fillings, nodules, etc., it is primarily composed of disaggregated and remoulded shale, silt, and sand weathered from the shale which is leached of highly soluble components (particularly when derived from marine shales such as the Mancos Shale: Laronne 1982).

Beneath the surface layer is a sublayer (crust) averaging about 5 to 10 cm in thickness which may range from a dense, amorphous crust (Hodges and Bryan 1982, Gerits *et al.* 1987) to a loose, granular layer (Howard 1970, Schumm and Lusby 1963). Part of the apparent variability of surface layer and crust may be due to differences among researchers in locating the division between these units. Below the crust there occurs a transitional 'shard layer' ranging from 10 to 40 cm in thickness consisting of partially disaggregated and weathered shale chips grading to firm, unweathered shale.

However, there is considerable variability in badland regoliths. Well-cemented sandstone layers outcrop as bare rock, often creating ledges or caprocks. Slightly cemented sand layers (often with $CaCO_3$ cement) generally form steep slopes with regolith 1 to 5 mm thick or less (Hodges and Bryan 1982, Bowyer-Bower and Bryan 1986, Gerits *et al.* 1987). Carman (1958) described a regolith in fluted badlands in a clay matrix-supported conglomerate com-

Figure 9.2 Rounded badland slopes in Morrison Formation.

posed of a hard veneer of sandy clay 1 to 15 cm thick over a softer interior layer and a hard core. Badlands on shaly sandstones in the Summerville Formation have a non-cohesive surface layer of sand grains and shale chips which grades fairly uniformly to unweathered bedrock within 10 to 20 cm. Some badland surfaces are cemented with a biological crust of algae or lichens (Yair *et al.* 1980, Finlayson *et al.* 1987). Badlands in marine shales, such as the Mancos Shale, may have salt recrystallization in the sublayers and local areas of salt surface crusts (Laronne 1982). Due to the frequent occurrence of rapid mass wasting on steep badland slopes, recently denuded areas have atypically thin regoliths with poor development of the surface layer.

Systematic variations in regolith properties may be associated with slope aspect. Churchill (1981), in a comparison of north- and south-facing slopes in Brule Formation Badlands (South Dakota), found the north-facing slopes to be more gently sloping, more densely rilled, with deeper regoliths, and characterized by infrequent mass-wasting involving much of the regolith (20 to 30 cm). By contrast, south-facing slopes have frequent shallow (3 to 10 cm thick) sloughing failures. Churchill suggested that slower evaporation promotes deeper infiltration on north-facing slopes. Yair *et al.* (1980) found north-facing slopes in the Zin badlands of the Negev Desert to have a rough, lichen-covered surface, a deeper regolith, few rills, and relatively high runoff and erosion. South-facing slopes are smoother, with greater runoff, frequent mudflows, and pipe development, but they experience less runoff erosion overall.

Weathering processes of badland regolith development involve relatively modest changes in mineralogy, since the source rocks are poorly lithified sedimentary rocks. Simple wetting may be sufficient to disaggregate the shale and disperse the clay minerals. For example, unweathered blocks of Morrison Formation smectitic shales will completely disaggregate and disperse within a few minutes to a few hours in just enough water to completely saturate the sample (this may be a considerable relative volume of water because of the pronounced swelling). Rapid slaking accompanies this disaggregation. The shallow regolith on these slopes testifies to the absorptive capacity and impermeability of the surface layers. On the other hand, samples of unweathered Mancos Shale, a marine shale with illite dominant, decompose more slowly, with less swelling and incomplete dispersion. A yellowish liquor of dissolved salts (mostly sodium and calcium sulphates: Laronne 1981, 1982) is produced, whose accumulation apparently inhibits further disintegration. Leaching of these solutes is apparently required for complete weathering, and salt concentrations decrease upwards within the regolith (Laronne 1982). Some clayey sandstones may have a calcite cementing which requires dissolution before erosion, and the regolith is only a few millimetres thick (Bowyer-Bower and Bryan 1986). On the other hand, marls composed of more than 50% calcite and gypsum may be essentially free from cementation. Consequently clay mineral dispersion is all that is required to form a disaggregated regolith (Imeson and Verstraten 1985, Finlayson *et al.* 1987). Some unconsolidated sediments require no weathering prior to entrainment by rainsplash and runoff, so that regoliths are absent or only seasonally present due to frost heaving (for example, the artificial Perth Amboy badlands studied by Schumm 1956a).

The physical and chemical properties of clay minerals, grain size distribution, density, and cementation affect the weathering by wetting and leaching, runoff characteristics, sediment and solute yields, and badland form. The properties of shales relevant to their erosional behaviour can be measured by a number of simple physico-chemical tests of cation-exchange capacity, solute extracts (concentration and chemistry), Atterberg (consistency) limits, vane shear strength, dispersion index, aggregate stability, and shrink–swell behaviour (Imeson *et al.* 1982, Hodges and Bryan 1982, Bryan *et al.* 1984, Gerits *et al.* 1987, Imeson and Verstraten 1988).

EROSIONAL PROCESSES ON BADLAND SLOPES

Discussion of slope erosional processes is conventionally divided into wash processes (runoff and rainsplash erosion) and mass-wasting (creep, sliding, and flowage). This discussion follows that division, although these processes are so interrelated and intergraded that such divisions are primarily for convenience.

Mass Wasting

The rounded slopes of the Morrison (Fig. 9.2), Chinle, and Chadron Formations have been attributed to the dominance of creep as a slope-forming process (Davis 1892, Schumm 1956b, Howard 1970). These formations contain clays with high dispersive and shrink–swell potential. The volume changes occurring during wetting together with the loss of bulk strength encourage downslope sag and creep of surface layers. Schumm (1963) found surface creep rates to be proportional to the sine of the slope

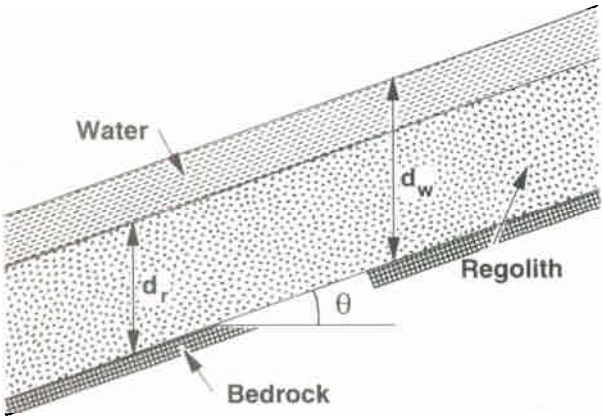

Figure 9.3 Definition of terms for infinite slope failure with water flowing parallel to the slope.

gradient for slope gradients less than 40° on Mancos Shale, and such a relationship is likely to be a good approximation to mass wasting rates for low slope gradients.

Many badland sideslopes are close to their maximum angle of stability, as long, narrow, shallow slips are common occurrences. Because these slopes are generally at angles of 40° or more, and failures occur during rainstorms, slope stability can be analysed by the well-known infinite slope model for saturated regolith and flow parallel to the slope (e.g. Lambe and Whitman 1969, pp. 352–6, Carson 1969, p. 87, Carson and Kirkby 1972, pp. 152–9). Figure 9.3 shows the definitions for an analysis similar to Lambe and Whitman's except that uniform surface flow is also allowed. Conditions for failure at a depth d_r below the surface are assumed to be approximated by a linear relationship

$$\tau_f = c + \sigma_e \tan\phi, \tag{9.1}$$

where τ_f is the shear stress on the failure plane, σ_e is the effective normal stress on the failure plane, c is the saturated cohesion, and ϕ is the saturated friction angle for the regolith material.

Based upon Figure 9.3 for the case when $d_w \geq d_r$ the shear and effective normal stresses on the potential failure plane are

$$\sigma_e = \rho_b d_r g \cos^2\theta \tag{9.2}$$

and

$$\tau = [\rho_t d_r + \rho_w(d_w - d_r)]g \sin\theta\cos\theta \tag{9.3}$$

where ρ_b and ρ_t are the buoyant and total densities of the regolith, respectively, ρ_w is the water density, g is the gravitational constant, θ is the slope angle, and d_w is the depth of water flow above the regolith surface. For the case when $d_w < d_r$

$$\sigma_e = [\rho_u(d_r - d_w) + \rho_b d_w]g\cos^2\theta \tag{9.4}$$

and

$$\tau = [\rho_u(d_r - d_w) + \rho_t d_w]g \sin\theta\cos\theta, \tag{9.5}$$

where ρ_u is the unsaturated unit weight of the regolith (which is likely to be very close to ρ_t).

Failure occurs when $\tau \geq \tau_f$. For the shallow badland regoliths only slight cohesion is necessary to permit slopes greater than 40° if water flow depths are small.

Wash Processes

Wash processes on badlands occur only during and immediately after rainstorms. If a rainstorm starts with a dry regolith (the usual case) much of the initial rainfall is absorbed by the regolith and initially penetrates deeply along cracks and between popcorn aggregates, where present. Runoff from badland slopes is delayed for several minutes after rainfall initiates; for example, Bryan *et al.* (1984) noted a delay of 10 to 15 minutes after initiation of sprinkling at a rate of 10 to 20 mm h^{-1}. The depth of wetting is limited either by absorption along crack and fissure edges or by ponding on top of the dense crust layer, where present (Hodges and Bryan 1982). Swelling of the regolith clays rapidly begins to close the cracks and gaps, so that flow is increasingly restricted to lateral flow in larger cracks and, in many cases, to micropipes developed near the crust–shard layer boundary (Hodges and Bryan 1982) (Fig. 9.4). The flow in the larger cracks, especially where appreciable flow is received from upslope, may be able to erode crack walls and keep pace with regolith swelling (Engelen 1973). Most of these cracks will form ephemeral rills, which are partly or wholly eradicated by continued swelling and subsequent drying and cracking of the surface layer. Sediment is added to the flow both by shear and dispersion of clay minerals, and the sediment load may range up to mudflow concentrations. Flow in the cracks and micropipes eventually feeds into rills or on to alluvial surfaces. Badland interflow has been compared to intergranular flow to drains (the rills) (Gerits *et al.* 1987, Imeson and Verstraten 1988) (Fig. 9.5). Through liquefaction of saturated, dispersed crust above the shard layer with accompanying runout, surface rills may initiate pipe formation and surface collapse in the zones of greatest depth of saturation between surface rills (Fig. 9.5).

Hodges and Bryan (1982) pointed out that in Dinosaur Badlands, Canada, runoff occurs more

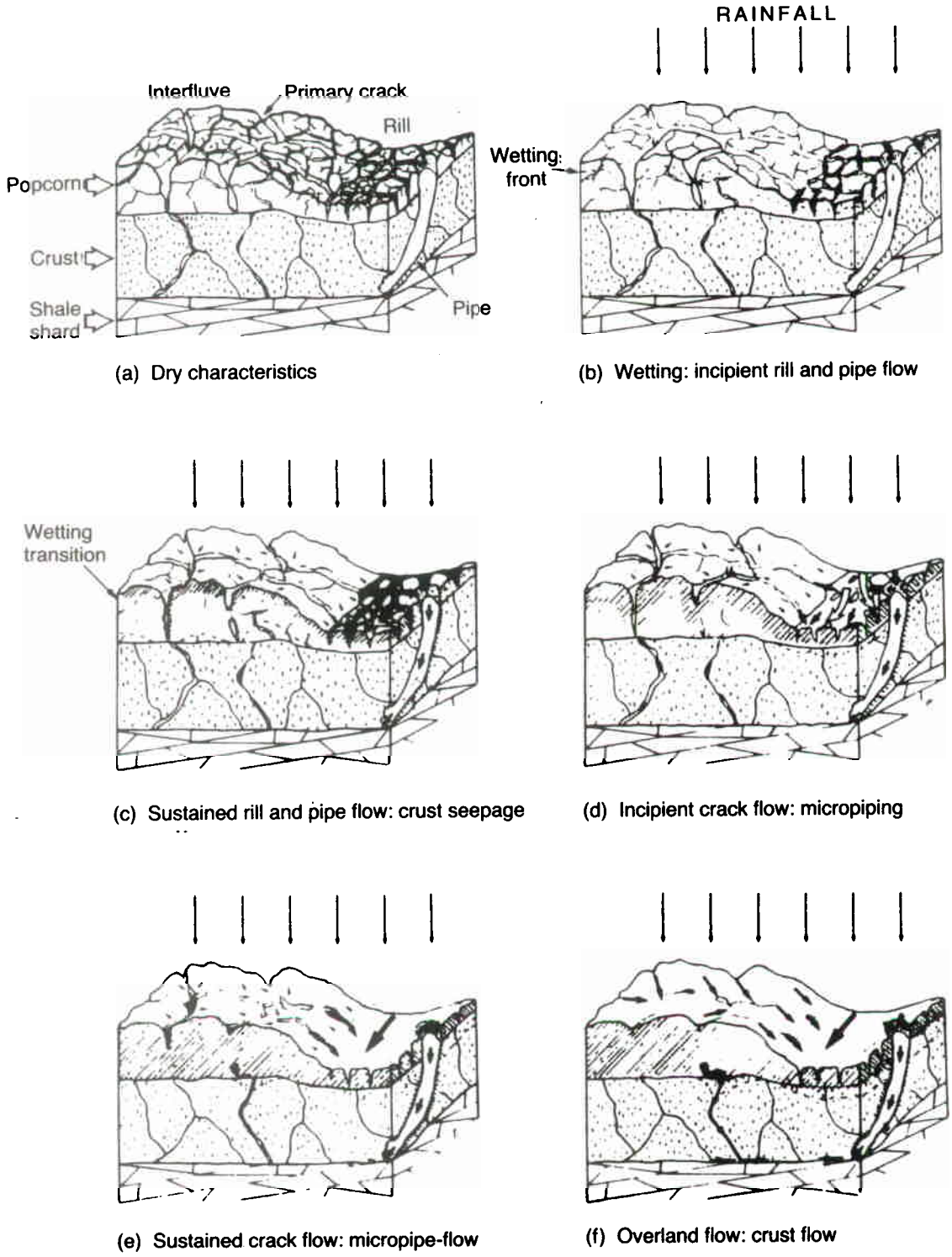

Figure 9.4 Regolith structure and runoff behaviour on shale badland slopes. Diagrams (a) through to (f) portray successive stages in wetting and runoff development (after Hodges and Bryan 1982).

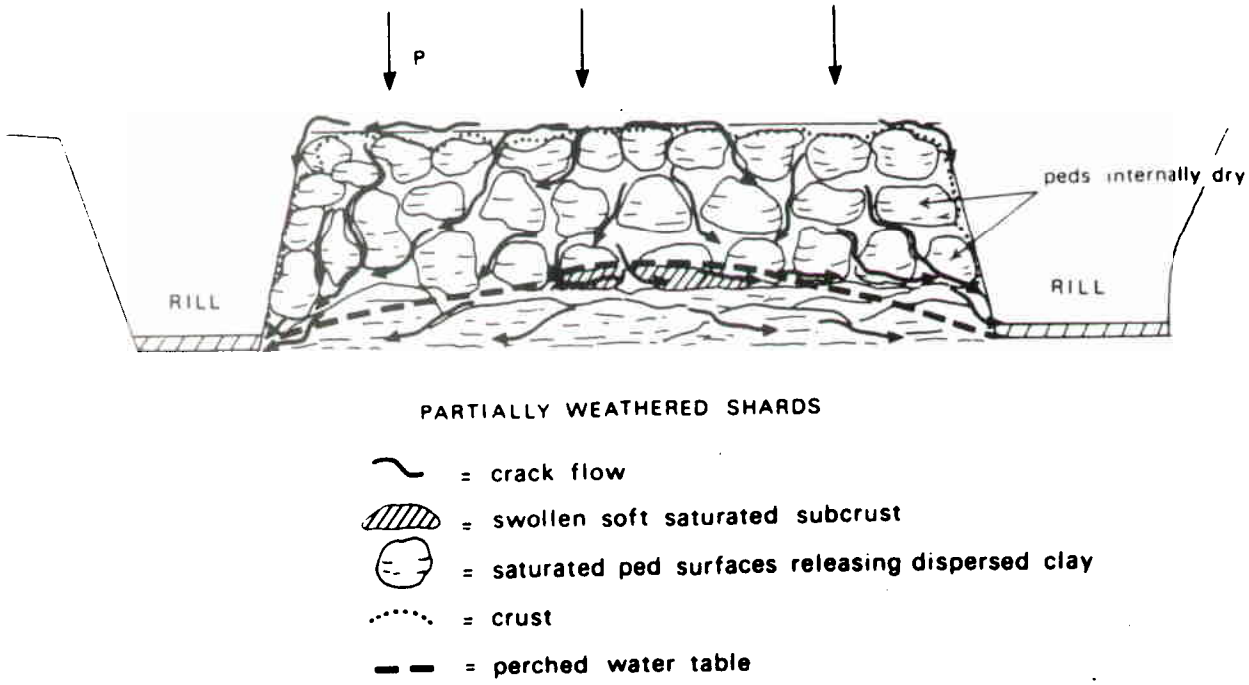

Figure 9.5 Development of a perched water table on top of shard layer in badland regolith and lateral drainage to rills. Note development of a saturated, soft layer between the rills which may fail, forming a pipe and eventually a new rill (after Imeson and Verstraten 1988).

rapidly and more completely on silty surfaces which locally encrust badland rills than on the cracked surface layers of badland slopes. Such silty layers in rills are uncommon on badlands in the Henry Mountains region, but alluvial surfaces are generally covered by such sediment and have rapid runoff response. A very few gentle badland slopes in Morrison Shale exhibit a banding alternating between typical popcorn-textured badland slopes and short alluvial surfaces (Fig. 9.6). The absence of shrink–swell cracking of the alluvial surfaces suggests that the silt layers are very effective at preventing infiltration. The banding may be an expression of layering in the shale or it may indicate a natural bifurcation at low slope gradient between normal badland slopes with swelling enhanced by water shed from upslope alluvial patches and alluvial surfaces graded downstream to the swollen shale bands.

In some badlands much of the slope drainage is routed through deep, corrasional pipe networks (see reviews by Harvey 1982, Campbell 1989, Jones 1990, Parker *et al.* 1990 and several papers in the volume edited by Bryan and Yair 1982b). Piping in susceptible lithologies is encouraged by prominent jointing and steeper hydraulic gradients via underground rather than surface paths caused by layering in the bedrock or through dissection of an originally flat upland (Campbell 1989). Piping is rare in the Henry Mountains badlands discussed here.

Rainsplash

Rainsplash erosion is important on badlands both as a direct agent of detachment and splash transport and indirectly as detachment contributes to runoff erosion and affects the flow hydraulics of shallow flows. A considerable experimental literature exists on rainsplash erosion mechanics (Chapter 8); the major controlling variables are raindrop size and velocity, rain intensity, and regolith characteristics. Few direct measurements exist of the contribution of rainsplash to badland slope erosion. Howard (1970) and Moseley (1973) attributed narrow, rounded divides on some badlands to the action of rainsplash rather than to creep (see below). Carson and Kirkby (1972, p. 221) also suggested that divide convexity may be caused by rainsplash on some arid slopes. The influence of rainsplash may be limited at the beginning of rainstorms by the cohesiveness of the dry clay, and biotic crusts, where present, protect shale regolith from rainsplash entrainment (Yair *et al.* 1980, Finlayson *et al.* 1987). In contrast to agricultural slopes, rainsplash has modest direct influence on overland flow hydraulics due to the concentration of flow into cracks and micropipes.

Figure 9.6 Low, terraced hillslope on shale in Morrison Formation. White bands are small segments of alluvial surface.

Runoff Erosion

Runoff on badlands seldom exemplifies the classic characteristics of overland flow on agricultural land because of the concentration of flow into cracks, micropipes, and ephemeral rills. The rate of erosion in such channelled overland flow and interflow, as well as in larger rills and washes, functionally depends upon flow conditions and resistance of the bedrock or regolith to weathering or detachment. The processes of erosion are poorly understood but may involve direct detachment from the bedrock, scour by sediment, and weathering processes such as leaching and wetting with dispersion.

Several approaches have been used to quantify runoff erosion in both rills and interrill areas. The most common approach on agricultural slopes is to estimate sediment transport rates using bedload or total load transport formulae assuming that the flow is loaded to capacity in the sand size ranges (transport-limited conditions). These are often empirically corrected for rainsplash effects based upon results of plot experiments in non-cohesive sediments or weakly cohesive soils (e.g. Meyer and Monke 1965, Komura 1976, Gilley *et al.* 1985, Julien and Simons 1985, Kinnell 1990, 1991, Everaert 1991). Detachment by rainsplash is assumed to assure capacity transport even where soils are moderately cohesive. Theoretical and empirical runoff erosion models commonly assume capacity transport (e.g. Kirkby 1971, Carson and Kirkby 1972, pp. 207–19, Smith and Bretherton 1972, Hirano 1975), but such assumptions often overestimate actual transport rates severalfold (Dunne and Aubrey 1986). Due to the cohesion and the small sand-sized component of badland regoliths, coupled with the steep slope gradients, runoff and interflow are likely to carry bed sediment loads well below capacity.

A few researchers have recognized that flow on steep slopes is commonly detachment-limited and suggest that the detachment (or deposition) by the flow D_f is related to an intrinsic detachment capacity D_c (for zero sediment load), the actual sediment load G and the flow transport capacity T_c (Foster and Meyer 1972, Meyer 1986, Lane *et al.* 1988, Foster 1990)

$$D_f = D_c(1 - G/T_c). \tag{9.6}$$

This relationship implies an interaction between

deposition and entrainment on the bed. However, rills and badland slopes seldom show evidence of sediment redeposition or partial surface mantling until flow reaches alluvial washes or alluvial surfaces (miniature pediments). The downstream transition from bare regolith to sand- and silt-mantled alluvial surfaces is generally abrupt (Schumm 1956a, b, Smith 1958, Howard 1970). The high roughness and possibly the greater grain rebound on badland regolith may make transport capacity greater than for an alluvial surface at the same gradient (Howard 1980). This suggests that on steep badland slopes and rills actual detachment D_f can reasonably be assumed to equal the intrinsic detachment D_c. This approach is used in the following models.

Howard and Kerby (1983) successfully related areal variations in observed rates of erosion of bedrock channels on shales to the pattern that would be expected if erosion rates were determined by dominant shear stress in the channel. Following Howard (1970), they suggested that erosion rate $\partial y/\partial t$ (detachment rate) is determined by shear stress τ:

$$\partial y/\partial t = K_c(\tau - \tau_c)^{\beta}, \tag{9.7}$$

where τ_c is a critical shear stress, β is an exponent, and the constant of proportionality K_c depends upon both flow durations and bedrock erodibility. Foster (1982) and Foster and Lane (1983) assume a similar relationship (with $\beta = 1$) for rill detachment capacity. Numerous experiments on fluvial erosion of cohesive deposits indicate scour rates that correlate with the applied shear stress (Parthenaides 1965, Parthenaides and Paaswell 1970, Akky and Shen 1973, Parchure and Mehta 1985, Ariathurai and Arulandan 1986, Kuijper *et al.* 1989). Assuming certain hydraulic geometry and resistance equations, and further assuming that the dominant values of shear stress greatly exceed the critical value, then equation 9.7 can be re-expressed as a function of local gradient S and contributing drainage area A_d:

$$\partial y/\partial t = K_e A_d{}^{\gamma} S^{\delta} \tag{9.8}$$

where the constant of proportionality K_e likewise depends upon flow durations and bedrock erodibility as well as constants in the hydraulic geometry equations. Theoretical values for γ and δ for the assumed hydraulic geometry relationships are 0.4 and 0.8, respectively, with observed values being 0.45 and 0.7. Seidl and Dietrich (1991) suggest stream power per unit channel length rather than shear stress may be the controlling factor for bedrock erosion. If so, $\delta = 1$ and γ is the exponent of proportionality between effective discharge and drainage area.

In some badland washes and in much of the throughflow in badland regolith the limiting factor may be the rate of decrease of shear strength of surface rinds either due to weathering of the bedrock or to wetting and dispersion of regolith crusts and shards. Even though the weathering rate is a limiting factor, flow conditions can still affect erosion rates, as illustrated in the following simple model.

Assume that the flow characteristically removes rinds or flocs of thickness δd and that the weathering at that depth decreases the shearing resistance c at a decreasing exponential rate from the initial shale cohesion c_i to a minimum value c_f:

$$c = c_f + (c_i - c_f)e^{-\lambda \delta t}, \tag{9.9}$$

where δt is the elapsed time since weathering has begun and λ is a characteristic weathering rate that depends upon wetting duration, bedrock or regolith permeability, and shale properties. Dislodgement of the weathered layer occurs when $\tau \geq c$, giving the time to dislodgement as

$$\delta t = \frac{1}{\lambda} \frac{(c_i - c_f)}{(\tau - c_f)} \tag{9.10}$$

Assuming that weathering begins anew when a layer is stripped by the flow and that τ_e is the effective shear stress, then the average erosion rate would be given by

$$\frac{\partial y}{\partial t} = \frac{\delta d}{\delta t} = \delta d\, \lambda / \ln \left[\frac{(c_i - c_f)}{(\tau_e - c_f)} \right] \tag{9.11}$$

Although this is a simplistic model, it does illustrate that if $\tau_e < c_f$ no erosion occurs; if $\tau_e > c_f$ there is a minimum erosion rate given by the weathering rate $\partial d\lambda$, and if $\tau_e > c_i$ the erosion rate is infinite. For the more interesting case of $c_i > \tau_e > c_f$ the erosion rate increases with τ_e, and where $c_i \gg \tau_e > c_f$ the rate of increase is nearly linear.

Both of these models suggest an erosion rate that increases with some measure of the strength of the effective flow. However, data on erosion rates in badland channels is limited, and that on the accompanying flow is essentially non-existent.

In some cases flows in bedrock rills may become so sediment laden that they exhibit Bingham flow properties (discussed in Chapter 8) with development of levees on rills and depositional mudflow fans. The common occurrence of localized slumps and draping flows on badland slopes might be

appropriately characterized by Bingham flow as well.

Requisite conditions for rill development and the overall control of drainage density in badlands has been a continuing theme in badlands geomorphology, starting with Schumm's (1956a) introduction of the 'constant of channel maintenance', a characteristic length from the divide to the head of rills. Rills have been discussed in two contexts. The first is the critical hydraulic conditions required for the transition from dispersed overland flow to channelized rill flow (see general discussions in Bryan 1987, Gerits *et al.* 1987, Torri *et al.* 1987, Rauws and Govers 1988). Several criteria have been proposed, including critical slope gradients (Savat and de Ploey 1982), a critical Froude number (Savat 1976, 1980, Karcz and Kersey 1980, Hodges 1982, Savat and de Ploey 1982), and a critical shear stress or shear velocity (Moss and Walker 1978, Moss *et al.* 1979, 1982, Savat 1982, Chisci *et al.* 1985, Govers 1985, Govers and Rauws 1985, Rauws 1987). On the steep badland slopes with strongly channelized flow in cracks, microrills, and pipes much of the flow exceeds critical conditions for rill initiation by any of these criteria. Rill initiation on badland slopes has also been related to unroofing of tunnels and micropipes (Hodges and Bryan 1982) which may be related as much to saturation, swelling, and softening of badland regolith as to the hydraulic factors mentioned above (see Fig. 9.5, Gerits *et al.* 1987, Imeson and Verstraten 1988).

Runoff thus seems to be capable of rill initiation over most badland slope surfaces, with the possible exception of sandstone layers with thin regoliths. The development and maintenance of semi-permanent rills require a balance between the tendency of runoff to incise and other processes that tend to destroy small rills (Schumm 1956a, Kirkby 1980). Such processes include shrink–swell of the surface layers, which destroys microrills (Engelen 1973), needle-ice growth (Howard and Kerby 1983), mass wasting by creep and shallow slides (Schumm 1956a, b, Howard and Kerby 1983), and rainsplash (Howard 1970, Moseley 1973, Dunne and Aubrey 1986). On badlands in humid climates a well-defined seasonal cycle of rill creation and obliteration occurs (Schumm 1956a, Howard and Kerby 1983). In arid regions advance and retreat of rill systems on slopes may occur over much longer timescales, but may also be dramatically altered by a single heavy summer rainfall or a winter mass wasting event. In the discussion below the emphasis is on 'permanent' rills and gullies that have persisted long enough to have created well-defined valleys. In the simulation modelling discussed at the end of the chapter, the location of permanent rills is determined by the balance between runoff erosion using equation 9.7 (with or without a critical shear stress) and diffusive processes (rainsplash or mass wasting).

BADLAND ARCHITECTURE AND EVOLUTION

The remainder of this chapter emphasizes the spatial process variations that determine the overall architecture of both slope and channel features of badlands. Furthermore, the temporal evolution of badlands will be examined both through reference to the specific case of the Henry Mountains area and through the use of simulation models.

EVOLUTION AND AREAL DISTRIBUTION OF BADLANDS

The rapid erosion of badland slopes means that they occur only where high relief has been created in shaly rocks. In the Henry Mountains area this has occurred through erosional removal of a protective caprock or through rapid master stream downcutting. The ramparts of sandstone cuestas feature local badlands in subcaprock shales, and more extensive badland areas occur where buttes have been recently denuded of their caprock. However, the badlands on cuesta ramparts are well developed only during relatively arid epochs (such as the present) when mass wasting of caprocks is relatively quiescent (see discussion in Chapter 7).

The master stream is the Dirty Devil–Fremont River system, which during the Quaternary has had a history of alternating stability or slight aggradation during pluvial epochs with rapid downcutting, followed by stability at the close of non-pluvial epochs (Howard 1970, 1986). During the pluvial epochs the stable base level coupled with physical weathering and mass wasting of the sandstone cuestas resulted in development of extensive talus slopes on the ramparts of the escarpments coupled with gravel-veneered alluvial surfaces (pediments) mantling the shales. Thus badlands were rare during pluvial epochs, probably occurring only locally on scarp ramparts or caprock-stripped buttes. The post-pluvial (Bull Lake) dissection of river terraces and alluvial surfaces underlain by Mancos Shale has created the spectacular badland landscape near Caineville, Utah (Fig. 9.1). The river apparently downcut about 65 m shortly after the close of the Bull Lake pluvial, followed by stability at about its present level (Howard 1970). As a result, a wave of dissection has moved headwards towards the sand-

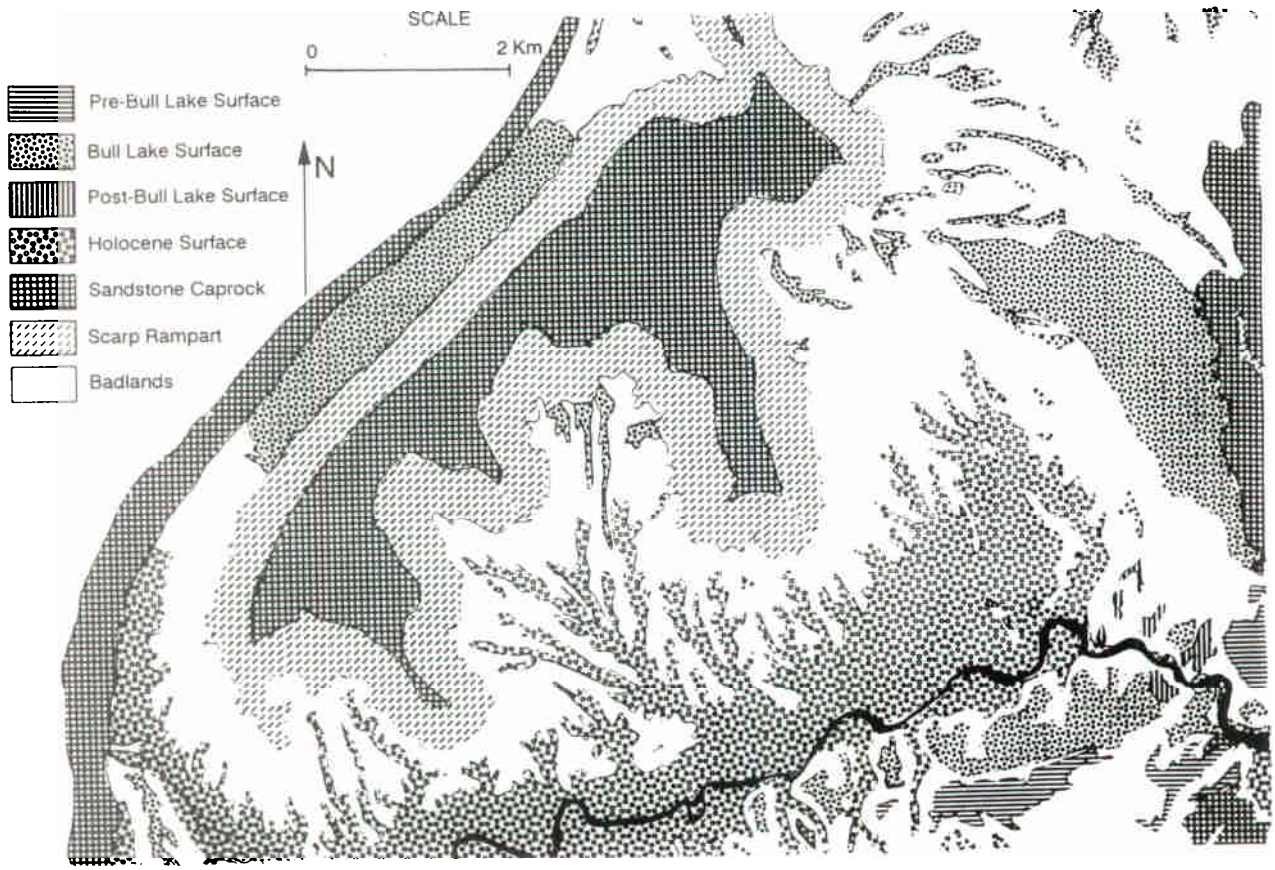

Figure 9.7 Geomorphic map of part of the Caineville Area, near the Henry Mountains, Utah. Bull Lake terrace may be early Wisconsin or Illinoian in age.

stone cuestas to which the alluvial surfaces were graded, producing a sequence of landforms from scattered Bull Lake alluvial surface remnants near the scarps (remaining primarily where the capping gravels were thickest) through a zone of high-relief (50 to 60 m) badlands to modern alluvial surfaces near the master drainage where the badlands have been completely eroded (Fig. 9.7). Shale areas that are either remote from the master drainage or have been protected from stream downcutting by downstream sandstone exposures are either undissected Pleistocene alluvial surfaces or very low-relief badlands.

Similar post-glacial downcutting has been implicated in forming the shale badland landscapes of the Great Plains of the United States and Canada (Slaymaker 1982, Wells and Guiterrez 1982, Bryan *et al.* 1987, Campbell 1989), with a similar progression from undissected uplands (often capped by a protective grassland cover) through high-relief badlands to modern alluvial surfaces. In semi-arid and humid regions, badlands occur primarily where a former vegetation has been removed from shales or easily eroded regolith. Thus such occurrences are similar to relief generation through a protective caprock and its subsequent removal.

FORM AND PROCESSES ON BADLAND SLOPES

Badlands exhibit a surprisingly wide range of slope form. A contrast between steep, straight-sloped badlands with very narrow divides and a convex form with generally gentler slopes was noted quite early in the literature on badlands and is exemplified in the classic South Dakota badlands by slopes in the Brule and Chadron Formations, respectively (Schumm 1956b). In the Henry Mountains area a similar contrast occurs between badlands on the Mancos Shale and those in the Morrison Formation (compare Figs 9.1 and 9.2). Badlands in the Summerville Formation are similar to the Mancos Shale badlands in having straight slopes and narrow divides, but they have significantly lower maximum slope gradients (Table 9.1). Many badlands have quite complicated slope forms due to contrasting lithology and interbedded resistant layers (e.g. the

Table 9.1 Comparison of slope angles (in degrees) on badlands in Mancos Shale, the Summerville Formation, and the Morrison Formation

Formation	*Angle-of-repose slopes*[a]	*Unstable slopes*[b]	*Average slope angle*[c]
Summerville	31.5	31.7	27
Mancos	32	34.8	40
Morrison	–	34.8	–

[a]Slopes constructed of unweathered shale shards.
[b]Constructional talus slopes of mass-wasted regolith below vertical cliffs in shale.
[c]Average gradient of long natural slopes in areas of moderate to high relief.

Dinosaur Badlands of Canada). Occasionally, pinnacle forms of badlands are found that are characterized by extremely high drainage density, knife-edge divides, and generally concave slope form (Fig. 9.8). The following discussion of badland erosional processes links these differences in slope form to variations in lithology and climate.

The broadly rounded upper slopes of the Morrison, Chinle, and Chadron Formations are probably due to creep processes (see above). The popcorn texture of surface aggregates allows relatively large relative movements of the aggregates as their edges become wet and slippery. However, lower sideslopes sometimes exceed 40°, locally resulting in rapid flowage of the popcorn surface layer off the slope. This results in long, narrow tracks of exposed subsoil on the lower slopes which rapidly develop a new surface layer of popcorn aggregates. Convex slopes develop through creep in any circumstance where the creep rate increases monotonically with slope gradient and where creep is the dominant erosional process; this was first elaborated by Davis (1892) and Gilbert (1909).

Even on these rounded slopes runoff erosion becomes increasingly important downslope, becoming dominant in rills and locally within shallow pipes and cracks in the thin regolith.

The Mancos badlands have a nearly linear profile with narrow, rounded divides, which range in width from less than 0.5 m in high-relief badlands to 1 to 2 m in low-relief areas (Fig. 9.1). Because of the very thin regolith on these narrow divides and a tendency for development of a shale-chip surface armouring, Howard (1970) and Moseley (1973), attributed

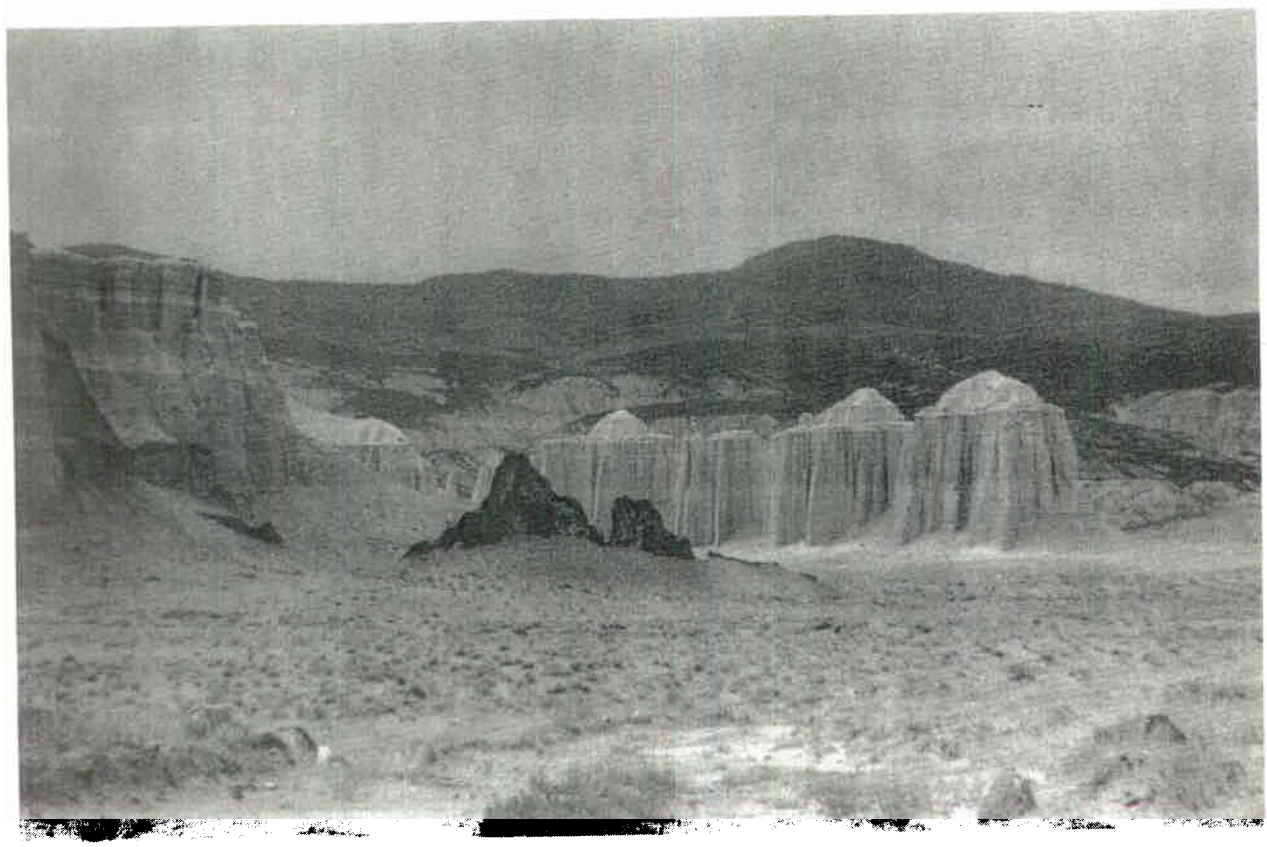

Figure 9.8 Pinnacle badland slopes in Cathedral Valley, near Caineville, Utah. The steep slopes were formerly protected by a caprock. Note the low-gradient slopes in the same formation (Entrada Sandstone).

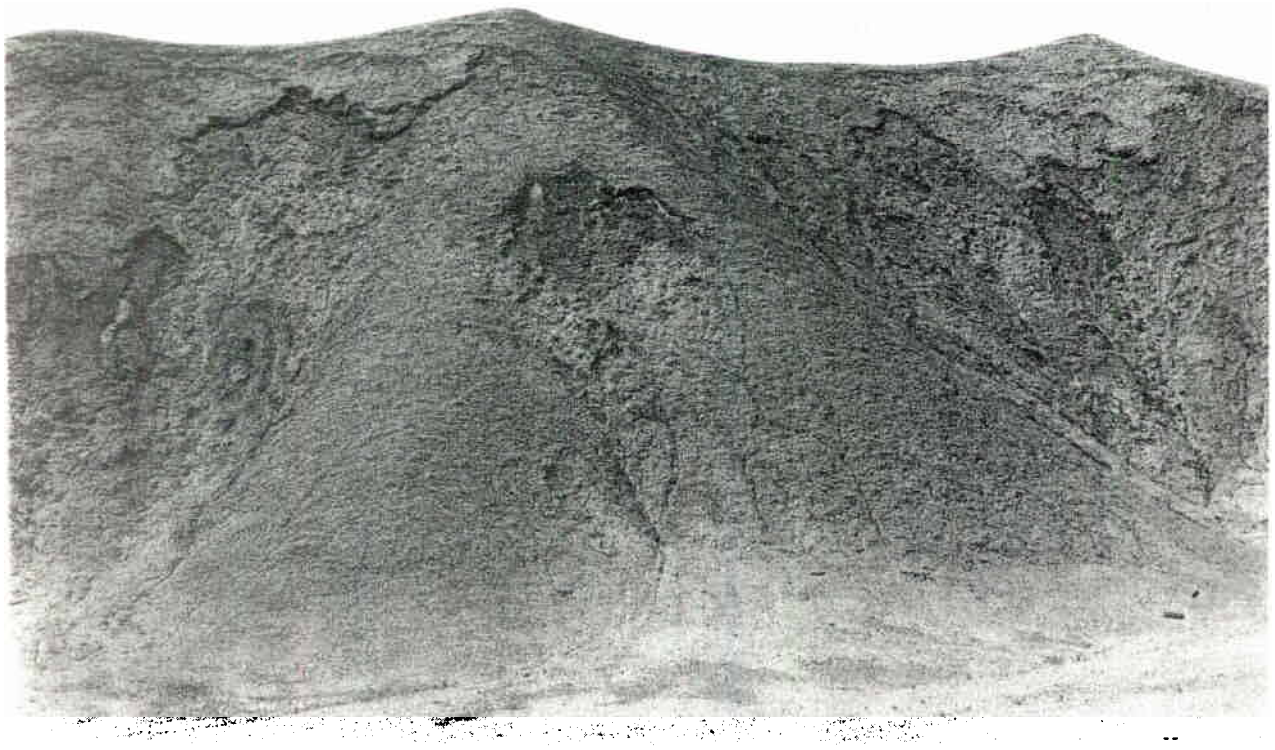

Figure 9.9 Meandering bedrock wash in Mancos Shale, showing undercutting of slopes and tendency for shallow slumping of undercut slopes.

the divide rounding to rainsplash. This process is effective on narrow divides even at low gradient because the maximum splash distance is greater than the divide width.

Virtually all high-relief badland slopes in the Henry Mountains region have nearly constant gradient on their lower portions, even on the broadly convex slopes in the Morrison Formation. These maximum gradients are usually within a few degrees of the angle of repose of dry detritus weathered from the formations. Maximum gradients on the Summerville Formation, with its loose weathered layer, are 3° to 5° less than the angle of repose, probably due to seepage flow decreasing the maximum stable slope angle (implied in equations 9.1 to 9.5; see Lambe and Whitman, 1969, p. 354). However, in the Morrison and Mancos badlands the slopes are 3° to 10° higher than the repose angle for loose weathered shale due to cohesion. Consequently, many lower slopes are on the verge of failing by flowage and slipping. Many such slopes do occasionally fail, involving only the thin surface layer (5 to 10 cm) and leaving long, narrow tracks of exposed subsoil on the lower slopes. Such flows are numerous on steep slopes on the Morrison and Summerville Formations but are rare on the Mancos badlands. However, on the Mancos badlands, whole sections of hillside appear to slip or slump short distances downhill during rainstorms, producing tension cracks arranged in waves suggesting differential movement and, rarely, extensive shallow slumping (Fig. 9.9). Tension cracks are the more numerous and wider the steeper the gradient, particularly on slopes undercut by meandering washes (Fig. 9.9).

On low-gradient portions of slopes, creep-like movement of the surface layer predominates. However, for the gradients approaching the limiting slope angle (which in actuality is temporally and spatially variable), mass wasting rates can be func-

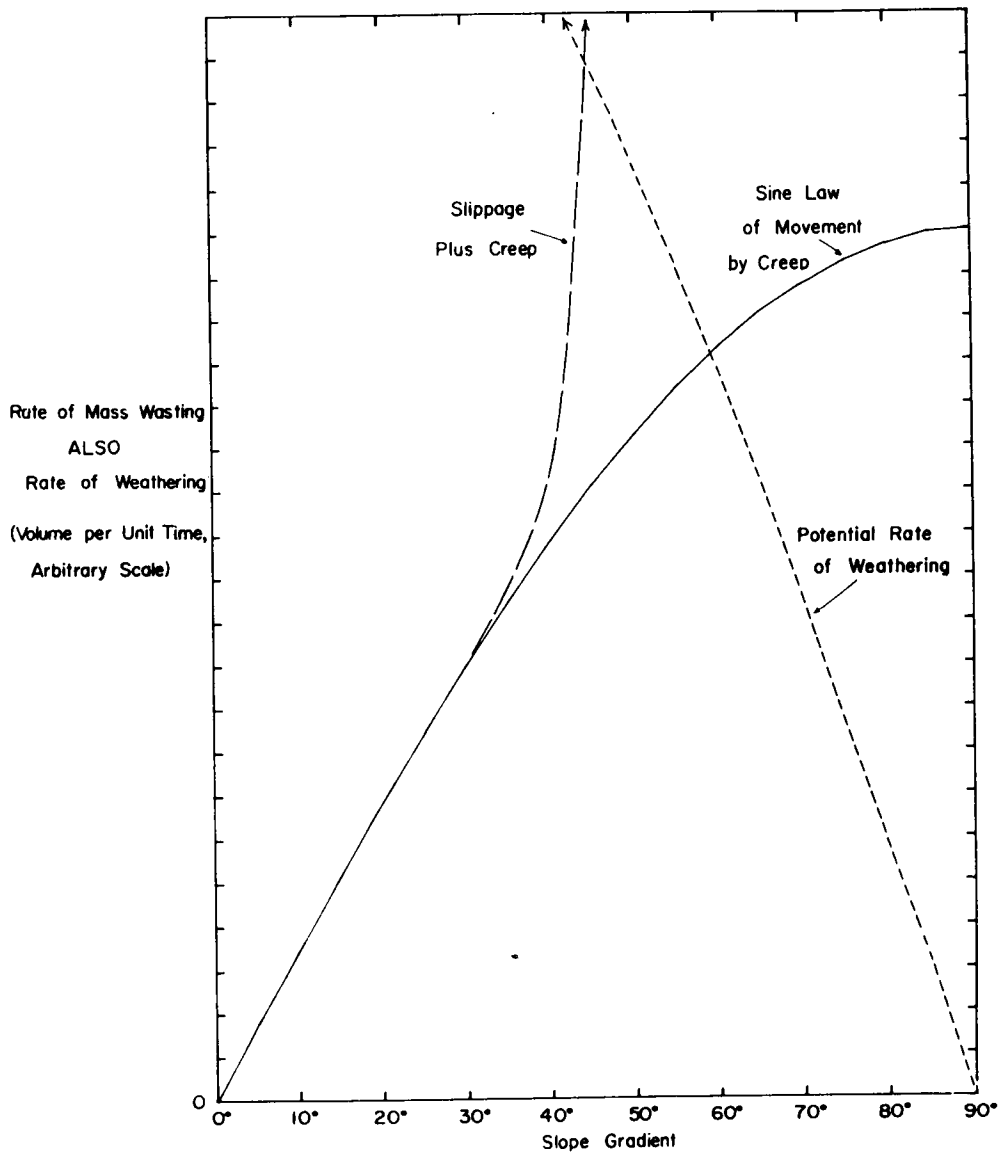

Figure 9.10 Conceptual plots of rate of mass wasting on badlands and potential rate of weathering as a function of slope gradient.

tionally represented by a rapid rate increase (Fig. 9.10). A similar approach was used by Kirkby (1984, 1985b).

Nearly linear lower slopes on regolith mantled, high-relief badlands would be expected if mass wasting determines slope form. Close to the divide, where creep rates are low (due to modest amounts of regolith supplied from upslope) and corresponding gradients are low, mass wasting rate follows the sine relationship. Consequently, gradients increase rapidly downslope. Rainsplash erosion is also a diffusive process, producing divide convexity. As a total volume of mass wasting debris increases downslope, equivalent rates of erosion may require gradients approaching the limiting slope angle where slippage or flowage becomes important. In these lower slope regions the incremental addition of weathered material along the slope can be accommodated by a very slight increase in gradient, thereby creating a nearly straight profile. Such lower slopes are essentially equivalent to the threshold slopes of Carson (1971) and Carson and Petley (1970), except that they are probably best modelled by a rapid but continuous increase in mass wasting rate as the limiting angle is approached rather than by an abrupt threshold.

Indirect evidence for threshold slopes in steep badlands comes from areal variations in badland

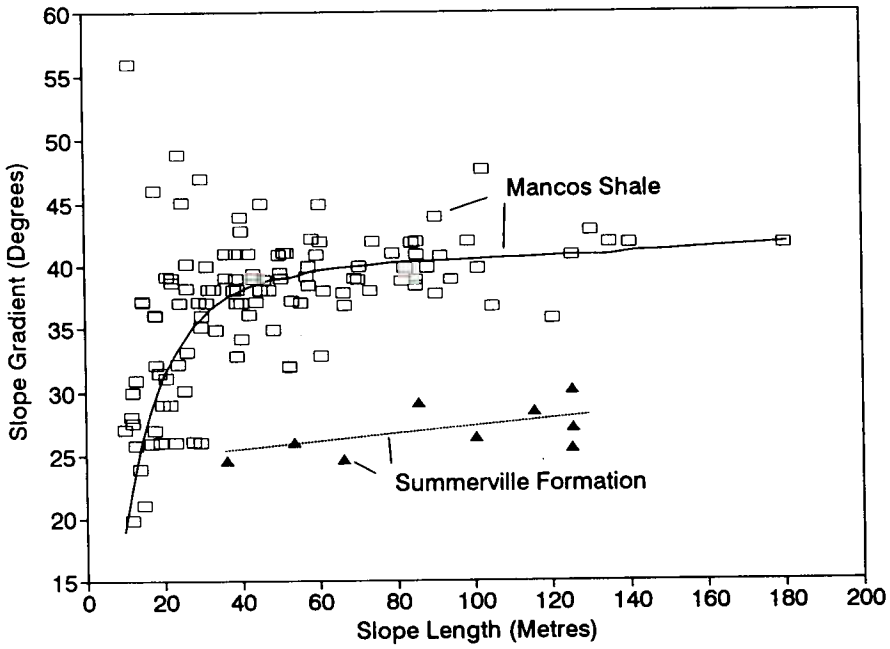

Figure 9.11 Plot of hillslope gradient versus slope length in badlands in the Summerville Formation and Mancos Shale.

form. Average hillslope gradients in badlands of the Summerville and Mancos Formations show little variation with slope length except for very short slopes (Fig. 9.11). However, the drainage density exhibits a complicated relationship to relief ratio, generally increasing with relief ratio up to a value of about 0.5, but decreasing in very high-relief badlands (Fig. 9.12). The relatively low drainage density of areas with very high relief ratio may be explained by the onset of sliding and slumping on steep slopes. In areas of high relief, large increases of the rate of erosion of a slope at its base should be accompanied by only a slight change in slope gradient (Fig. 9.10). But the small increase in slope angle increases the efficiency of erosion on the slope relative to the channel, so that the critical drainage area necessary to support a channel increases, with a resulting decrease in drainage density. Average slope length L and drainage density D are related to the average slope angle θ by (Schumm 1956a, p. 99)

$$L\cos\theta = 2/D. \qquad (9.12)$$

Because slope angles vary little with relief ratio in steep badlands, the decrease in drainage density accompanying increase in relief ratio is accompanied by a proportional increase in slope length. By contrast, in areas of low overall gradient, increase in relief ratio is accompanied by increases in drainage density. Therefore, slope length decreases nearly in proportion, since the cosine term is near unity.

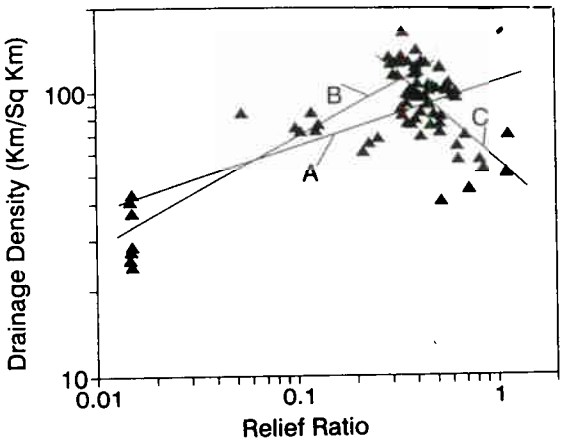

Figure 9.12 Drainage density versus relief ratio for badland areas in the Mancos Shale. Least-squares regression lines (A) for the data as a whole, (B) for values of relief ratio less than 0.35, and (C) for values greater than 0.2. Drainage density and relief ratio measured from aerial photographs with scale of 1:12 000. Each point represents measurement of a circular quadrat with radius of 150 m centred on a major badland divide. The relief ratio is defined from the quadrat centre to the lowest point on the quadrat circumference.

At least four types of surfaces occur on badlands: (a) slopes with exposed bedrock; (b) regolith-mantled slopes; (c) rills and washes with exposed bedrock; and (d) alluvium-mantled surfaces. These surfaces generally sharply abut against each other, with

Figure 9.13 Near-vertical slopes in shales of the Morrison Formation formed by past undercutting by the Fremont River. Differences in bedding are strongly expressed in vertical slopes in contrast to the smoother, gentler slopes mantled by 20+ cm of regolith.

the transitions corresponding to thresholds in the relative importance of processes. Most badland slopes are regolith-mantled, albeit shallowly. However, on steep slopes or where bedrock is resistant to weathering, regolith is absent and the surface is irregular, expressing variations in weathering characteristics of the rock, jointing, and stratigraphy (Fig. 9.13). In contrast, minor differences in lithology of the rocks underlying regolith-mantled badlands (non-undercut areas in Fig. 9.13) do not affect slope form, for the geometry is determined by processes of downslope transport of the weathered debris. The threshold between bare and regolith-mantled slopes is commonly equated with weathering- versus transport-limited conditions, respectively (Culling 1963, Carson and Kirkby 1972, pp. 104–6). However, there are four factors that may limit overall slope erosion rate, the potential weathering rate PW, the potential mass wasting rate PM, the potential detachment rate by runoff (combined splash and runoff detachment) PD, and the potential fluvial transport rate PT. On regolith-mantled slopes $PW > (PM + PD)$ and $PD < PT$. Either mass wasting or runoff detachment may be quantitatively dominant on such slopes; measurements by Schumm (1963) suggest runoff dominance. The use of the term transport-limiting for these mantled slopes is inaccurate, because the runoff component of erosion is detachment- rather than transport-limited. Bare bedrock slopes have $PW < (PM + PD)$ and $PD < PT$, so that the term weathering-limiting is appropriate. Alluvial surfaces have $PD > PT$, and generally $PM \approx 0$ because of the low gradients. Bedrock-floored rills and washes have similar conditions to bare rock slopes except that $PM \approx 0$. The rock-mantled slopes considered in Chapter 8 would appear to be similar to badland regolith-mantled slopes. However, the surface layer is often a lag pavement that greatly restricts runoff erosion, so that the overall rate of erosion is often determined either by (a) the rate of breakdown of the pavement by weathering or (b) the rate of upward migration of fines due to freeze–thaw or bioturbation, or (c) mass wasting rates.

The supply of moisture is the primary factor determining the weathering rate of the soft rocks forming badlands. For vertically falling precipitation the interception per unit surface area of slope diminishes with the cosine of the slope angle (in actuality some water attacks vertical or overhanging slopes, for escarpment caprocks often project beyond underlying shales). This suggests that overall slope erosion rates on badlands follow the relationships shown in Figure 9.10, where a critical gradient separates mantled slopes on which rates of mass wasting increase with slope gradient from steeper bedrock slopes which erode less rapidly as gradients increase (at least until slope relief is great enough to cause bulk failure in the shale bedrock).

Badlands with steep slopes and exposed bedrock commonly develop pinnacle forms (alternatively termed needle-like, serrate, or fluted) (Fig. 9.8). Examples include the Brice Canyon pinnacles, the badlands described by Carman (1958), the spires of Cathedral Valley, Utah, and portions of the badlands of South Dakota. Pinnacle badlands commonly are initiated as a result of near-vertical slopes developing in non-resistant shales lying beneath a resistant caprock which erodes very slowly as compared with downwearing in the surrounding badlands. Eventually the caprock is weathered away or fails, and the underlying shales rapidly erode, developing the fluted form due to rapid rill incision because of the steep relief. Drainage densities are exceedingly high on these slopes and, owing to the absence of a mantling regolith and mass wasting processes, divides are knife-edged. Slope profiles are generally concave, indicating the dominant role of runoff (both unconcentrated and in rills) in erosion. Although the steepness of the fluted slopes is partially due to the high initial relief, the slopes at divides generally steepen during development of fluted badlands because rill erosion rapidly erodes slope bases and weathering and erosion rates on sideslopes *decrease* with increasing slope gradient (Fig. 9.10). As the fluted slopes downwaste, they are generally replaced by mantled badland slopes with lower drainage density at a very sharp transition (Fig. 9.8).

FLUVIAL PROCESSES AND LANDFORMS OF BADLAND LANDSCAPES

Howard (1980) distinguished three types of fluvial channels: bedrock, fine-bed alluvial, and coarse-bed alluvial. In most cases these types of channel are separated by clear thresholds in form and process. In badlands coarse-bed alluvial channels usually occur only where gravel interbeds are present.

Alluvial Surfaces

Few contrasts in landscape are as distinct as that between badland and alluvial surfaces on shaly rocks. Low-relief, alluvium-mantled surfaces in badland areas have been referred to by a variety of names, including miniature pediment (Bradley 1940, Schumm 1956b, 1962, Smith 1958), pseudo- and peri-pediment (Hodges 1982), and alluvial surface (Howard 1970, Howard and Kerby 1983). The last term is used here because of its neutral connotation regarding the numerous and conflicting definitions of pediment.

Flow on alluvial surfaces is either unconfined or concentrated in wide, braided washes inset very slightly below the general level of the alluvial surface (Fig. 9.14). Alluvial surfaces may be of any width compared with that of the surrounding badlands, contrasting with the confinement of flow in bedrock rills and washes. The alluvium underlying most alluvial surfaces is bedload carried during runoff events and redeposited as the flow wanes, but adjacent to major washes overbank flood deposits may predominate. Although the surface of alluvial surfaces and washes is very smooth when dry, during runoff events flow is characterized by ephemeral roll waves and shallow chute rilling which heals during recessional flows (Hodges 1982).

An alluvial surface and badlands commonly meet at a sharp, angular discordance (Fig. 9.15). At such junctures slopes, rills and small washes with inclinations up to 45° abut alluvial surfaces with gradients of a few degrees. In most instances the alluvial surfaces receive their drainage from badlands upstream and are lower in gradient than the slopes or washes. The layer of active alluvium beneath an alluvial surface may be as thin as 2 mm, but increases to 10 cm or more below larger braided washes. Below the active alluvium there occurs either a thin weathered layer grading to bedrock or, in cases where the alluvial surface has been aggrading, more alluvium.

Generally alluvial surfaces and their alluvial washes obey the same pattern of smaller gradients

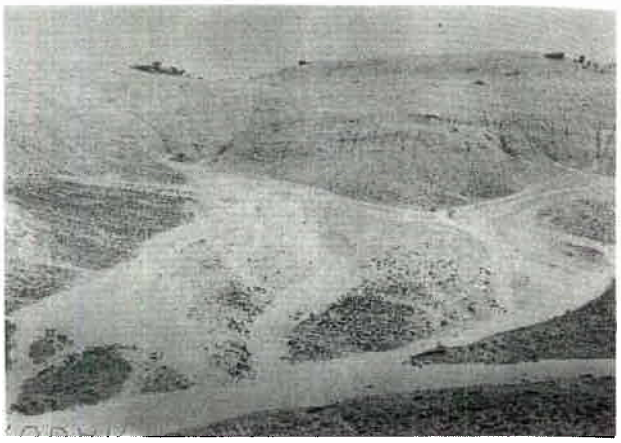

Figure 9.14 Runoff on alluvial surfaces on Morrison Formation Shales. Photo was taken during waning flow stages.

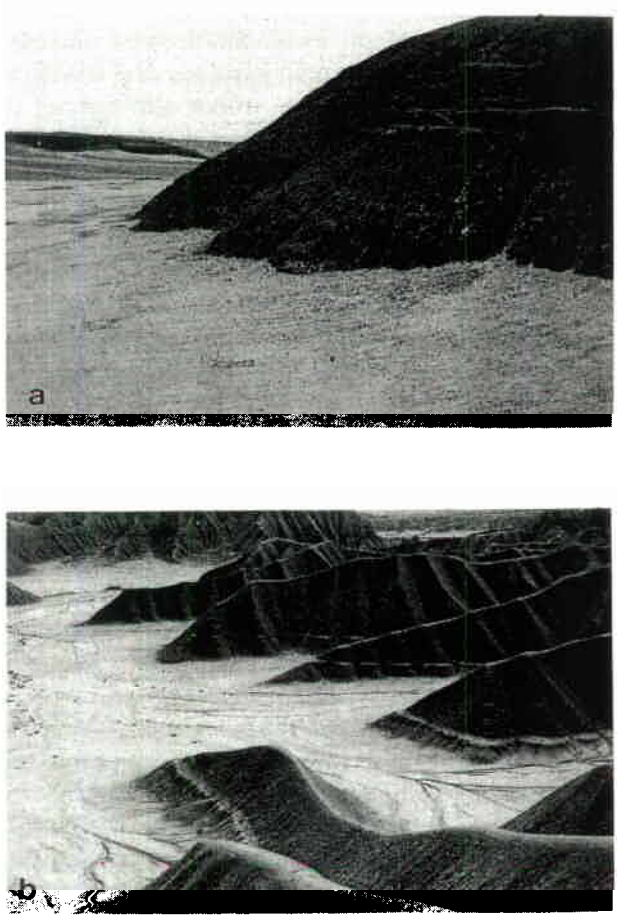

Figure 9.15 Sharp junction between steep badland slopes and alluvial surface (a and b).

Figure 9.16 Badlands and dissected alluvial surface in Mancos Shale. The former boundary between badland slopes and the alluvial surface occurred at the light–dark transition.

for larger contributing areas. Howard (1970, 1980) and Howard and Kerby (1983) showed that the gradient of alluvial surfaces is systematically related to the contributing drainage area per unit width (or equivalent length) A_L in badlands both in arid and humid climates:

$$S = CA_L^z \tag{9.13}$$

where the exponent z may range from -0.25 to -0.3. The equivalent length for washes on alluvial surfaces is simply the drainage area divided by the channel width, but for unconfined flow on smaller alluvial surfaces it is the drainage area contributing to an arbitrary unit width perpendicular to the gradient. The proportionality constant C can be functionally related to areal variations in sediment yield, runoff, and alluvium grain size. Howard (1980) and Howard and Kerby (1983) showed that the value of the exponent z is consistent with the assumption that alluvial surface gradients are adjusted to transport sand-sized bedload at high transport rates.

Badland alluvial surfaces are therefore comparable to sand-bedded alluvial river systems in general in that gradients decrease with increasing contributing area (downstream). The major contrast is the presence of unchannelled areas in the headward portion of alluvial surfaces. Their presence is probably related to the absence of vegetation and flashy flow, which discourages formation of banks and floodplains. The alluvial surfaces contrast with alluvial fans in that the former are through-flowing systems with only minor losses of water downstream and contribution of water and sediment from the entire drainage area. Furthermore, the alluvial surfaces are generally slowly lowering. If they are aggrading, they do so at a very slow rate. Thus the downstream spreading of discharge characteristic of alluvial fans (and deltas) generally does not occur on alluvial surfaces.

Alluvial surfaces are surfaces of transportation, with a gradient determined by the long-term balance between supplied load and discharge (Smith 1958). Thus they are graded surfaces in the sense of Mackin (1948). Howard (1982) and Howard and Kerby (1983) discussed the applicability of this concept in the context of seasonal and long-term changes in the balance of sediment load and discharge, and the limits to the concept of grade. Interestingly, most badland alluvial surfaces slowly lower through time, as indicated both by direct measurements (Schumm 1962, Howard and Kerby 1983) and by the presence of rocks on pedestals of shale surrounded by an alluvial surface that has lowered around it. Thus the alluvial surfaces are not destroyed by slow lowering of base level, but they become readily dissected by bedrock washes if base level drops too rapidly (Fig. 9.16). Howard (1970) and Howard and Kerby (1983) presented evidence that larger alluvial channels are capable of more rapid erosion than smaller ones without being converted to bedrock channels. Howard and Kerby (1983) suggested that the maximum erosion rate is proportional to about the 0.2 power of drainage area. It is uncertain whether the erosion (or aggradation) rate on alluvial surfaces systematically influences their gradients.

Bedrock Channels

Badland washes and rills are usually floored by slightly weathered bedrock. Beneath the smallest

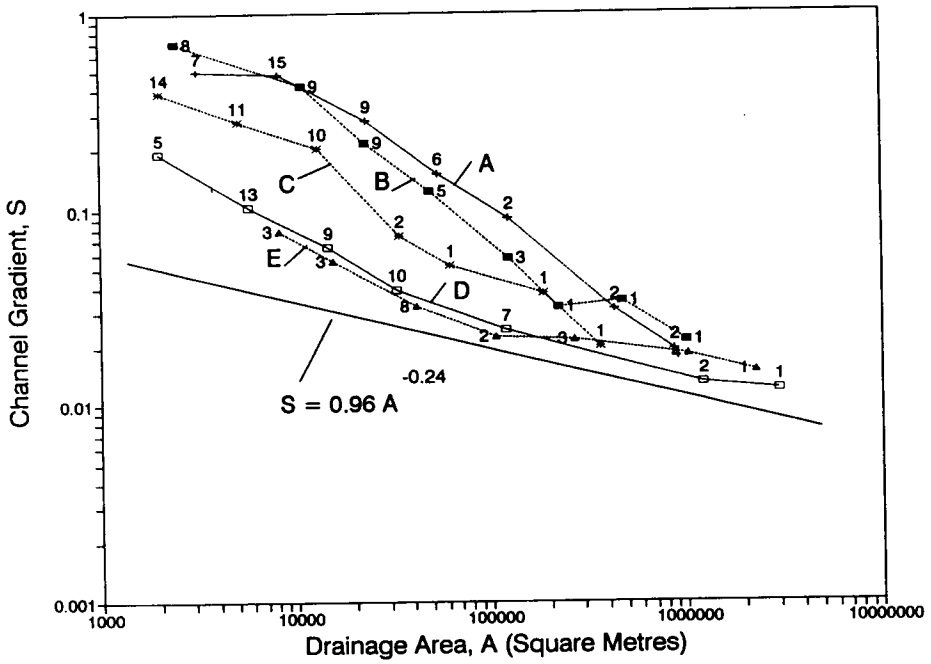

Figure 9.17 Relationship between size of drainage area and stream gradient for selected basins in the Mancos Shale near Caineville, Utah. Figures beside points show number of sample points that are averaged for clearer presentation. For comparison, the relationship between gradient and drainage area for alluvial surfaces on the Morrison Formation is shown.

rills the weathered zone is about as thick as that on adjacent unrilled slopes, although this thickness varies with the seasonal rill cycle (Schumm 1956a, 1964, Schumm and Lusby 1963). In larger badland washes, weathering products are rapidly removed, exposing bedrock. Deposits of alluvium occur only locally in scour depressions.

Larger bedrock washes often display marked meandering (Fig. 9.1) with the wavelength increasing systematically with the 0.4 power of drainage area (Howard 1970), which is consistent with meander wavelength in alluvial streams.

In contrast to the alluvial surfaces, the gradient of bedrock washes is not uniquely related to the size of contributing drainage area and their gradient is steeper than alluvial washes of equivalent area (Howard 1970, Howard and Kerby 1983). Figure 9.17 shows this relationship for bedrock badland drainage basins in the Mancos Shale near Caineville, Utah. Steep-gradient wash systems (A and B in Fig. 9.17) are either locations of complete dissection of the Pleistocene alluvial surface or locations recently denuded of a protective caprock. Low-gradient bedrock wash systems (D and E in Fig. 9.17) occur where dissection of the Pleistocene alluvial surface has been inhibited by a high local base level in the form of a resistant rock unit. The gradients for all of the basins converge for high drainage areas, because the downstream ends of these wash systems are generally alluvial surfaces.

Slope–Channel Interactions in Badlands

Erosion in large bedrock streams may be nearly independent of the sediment load supplied by slope erosion (e.g. equations 9.7 and 9.11), so that the nature of the surrounding slopes has minor influence on stream erosion rates. Thus, in general, evolution of hillslopes follows rather than leads that of the stream network.

However, the low-order tributaries, including rills, interact with adjacent slopes and their gradients are largely determined by hillslope gradients. The smallest rills are ephemeral (Schumm 1956a, Schumm and Lusby 1963, Howard and Kerby 1983) and have gradients essentially equal to hillslope gradients.

The nature of hillslope–channel interactions is poorly understood. Permanent channels occur only where runoff is sufficient such that streams erode as rapidly as the surrounding slopes and with a lesser gradient. Diffusive processes (creep and rainsplash) are more efficient than channel erosion for small contributing areas. This is suggested by models of bedrock channel erosion (e.g. equation 9.8) where,

for a given erosion rate, gradients would have to approach infinity as contributing area approaches zero. In contrast, mass wasting slope processes and rainsplash function even at divides. Ephemeral rills are generally not inset into the slope because seasonal (or year-to-year) mass wasting by needle ice or shallow slips and direct frost heaving episodically destroys them. Permanent rills and washes are distinguished by (and can be defined by) being inset within a definable drainage basin, so that they have a lower gradient than surrounding slopes. Even so, such permanent rills may occasionally be partially infilled by mass wasting debris.

The sharpness of the junction between badland slopes and adjacent alluvial surface (e.g. Fig. 9.15) as well as its spatio-temporal persistence has fascinated generations of geomorphologists, and a variety of hypotheses have been offered for its origin and maintenance. Badlands rising from alluvial surfaces have gradients nearly equal to nearby slopes terminating at bedrock channels (Fig. 9.18), implying nearly equal rates of erosion, even though the alluvial surfaces may be stable or very slowly degrading. Moreover the slope form (straight-sided or broadly convex) remains the same. In Figure 9.18 successive profiles across the valley in a downstream direction may be similar to changes in profiles through time at one location, assuming that the alluvial surface remains at a stable level. The alluvial surfaces expand at the expense of the adjacent slope, as measured by Schumm (1962).

Schumm (1962), Smith (1958), Emmett (1970), and Hodges (1982) suggested that the abrupt contact is created and maintained by erosion concentrated at the foot of the slope, due perhaps to spreading of discharge from the rills at the base of the slope (a type of lateral planation), re-emergence of interflow, and changes of flow regime (subcritical to supercritical) at the slope–alluvial-surface junction. Engelen (1973) suggested that spreading of water emerging on to alluvial surfaces from ephemeral microrills may be as important as spreading flow from more permanent rills. Hodges (1982) provided experimental information and observations on flow on badland slopes, rills, and alluvial surfaces. These data indicate the complicated nature of flow on these surfaces, including ephemeral rilling of the alluvial surface.

Howard (1970) suggested that the abrupt change of gradient at the head of an alluvial surface can be maintained without recourse to special processes acting at this location. Simulation modelling of coupled bedrock and alluvial channel evolution (using an equation similar to equation 9.8 for bedrock erosion) indicated that bedrock channels maintained a nearly uniform gradient as they downcut until they were abruptly replaced by alluvial surface when elevations dropped to the level that the gradients were just sufficient to transport supplied alluvium (Figs 9.23 and 9.24, discussed below). Although these simulations were targeted to the bedrock channel system on badlands, a similar situation may pertain to unrilled badland slopes. Water erosion is the dominant erosional process at the base of badland slopes (Schumm and Lusby 1963) and may be governed by similar rate laws as permanent rills and washes. As noted above, most seemingly unrilled badland slopes are primarily drained by concentrated flow either through an ephemeral surface network of crack flows (which are obliterated during the swelling and reshrinking of the surface layer) or as interflow in deeper cracks and micropipes.

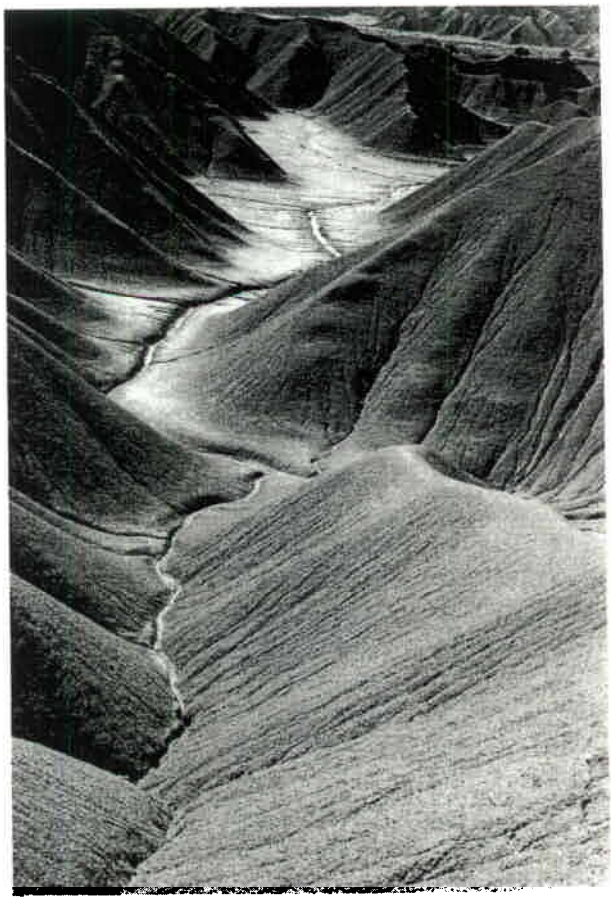

Figure 9.18 Downstream transition between bedrock wash and alluvial surface. Slope gradients are about the same whether grading to bedrock wash or alluvial surface.

Theoretical Models of Badland Evolution

There has been a rich history of quantitative modelling of slope and channel processes. These models

have not primarily been directed towards specific issues related to badland slopes, but they have a general formulation that could be adapted to specific processes and materials in badlands. Early models were primarily applied to evolution of slopes in profile only, either for ease of analytical solutions or for numerical solutions with modest computational demands. A variety of approaches have been used, but two end members can be identified. Some investigators, as exemplified by the approaches of Kirkby (Kirkby 1971, 1976a, b, 1985a, b, Carson and Kirkby 1972), have attempted to quantify almost all of the processes thought to be acting on slopes and their distribution both on the surface and throughout the regolith. This approach offers the promise of detailed understanding of the spatio-temporal evolution of regolith and soils as well as the potential for addressing site-specific issues of erosion processes, slope hydrology, surface water geochemistry, and soil and water pollution. Some attempts have been made to apply such models to cover areal as well as profile characteristics of slopes, including issues of initiation of drainage (Kirkby 1986, 1990). However, the generality of such models restricts their use over large spatial or temporal domains due to present limitations of computer resources and the large number of parameters that must be specified.

Another approach has been to deliberately simplify models in order to address issues of drainage basin morphology and landscape evolution. Ahnert (1976, 1977) has been a pioneer in developing three-dimensional models of landscape evolution, although most of his efforts have been directed to cross-sectional evolution of slope profiles (Ahnert 1987a, b, 1988). Recent advances in computer capabilities have permitted more general modelling of drainage basin evolution. The model of Willgoose *et al.* (1991a, b, c) was formulated to examine long-term evolution of drainage basin morphology through combined slope and channel process. Modelling with deliberately simplified process assumptions, they assume a combination of diffusional processes (such as creep or rainsplash erosion) on regolith-mantled slopes and sediment transport through a fine-bed alluvial stream network. Diffusion is modelled by a linear function of local slope gradient, and fluvial sediment transport rate is parameterized as a function of drainage area and channel gradient by assuming appropriate equations of hydraulic geometry and sediment transport rates.

A similar approach has been taken by Howard (in preparation) to examine variations in slope and drainage network geometry as a function of model parameters. This model is based upon the observation that drainage basins result from simultaneous action of diffusional and concentrative processes. For example, creep, rainsplash, and possibly some forms of overland flow (Dunne and Aubrey 1986) are diffusional, whereas most fluvial processes (excepting those on fans and deltas) are concentrative. The simulation model reported here includes creep (diffusional) and runoff (concentrative) erosion. The model was not specifically constructed to represent badland slopes. In particular, the model assumes gradients of only a few degrees such that $\sin\theta \simeq \tan\theta = S$ and $\cos\theta \simeq 1$. Weathering is assumed not to be a limiting factor and is not explicitly modelled. Creep is assumed to be limited to surface soil layers and thus is independent of total soil depth. The creep flux $\mathbf{q}$ is a function of the slope gradient $\mathbf{S}$:

$$\mathbf{q} = K_s \mathbf{S}^{\alpha} + K_t/(1 - C_t S^{\varepsilon}), \qquad (9.14)$$

where K_s and K_t are rate constants, α and ε are constant exponents, and a constant $C_t > 0$ allows for threshold-limiting slopes (bold type indicates vector quantities). The rate of erosion due to creep E_s equals the divergence of creep:

$$E_s = \nabla \cdot \mathbf{q}. \qquad (9.15)$$

Channels and rills are assumed to be bedrock-floored, with channel erosion rate E_c depending upon overland flow shear stress τ as given by equation 9.7, which is parameterized as a function of drainage area and local gradient (equation 9.8). The assumption of bedrock-floored channels means that explicit sediment routing in channels is not required. It also means that the development of alluvial washes and alluvial surfaces cannot be simulated with the present version of the model.

The total erosion at any location E_t is given by:

$$E_t = \begin{cases} E_s & \text{if } E_c = 0 \\ E_s/\eta + E_c & \text{if } E_c < 0 \end{cases} \qquad (9.16)$$

where $\eta > 1$ models the easier erosion of soil debris than bedrock.

Simulations have been conducted with this model on a 100×100 matrix. The simulations generally assume that the bottom boundary is a horizontal outflow which is lowered at a constant rate E_b so that a steady state topography gradually develops. The top boundary is a drainage divide, and the side boundaries are periodic (elevations on the left boundary are continuous with those on the right, and soil or water leaving the left boundary enters at the same relative position at the right boundary).

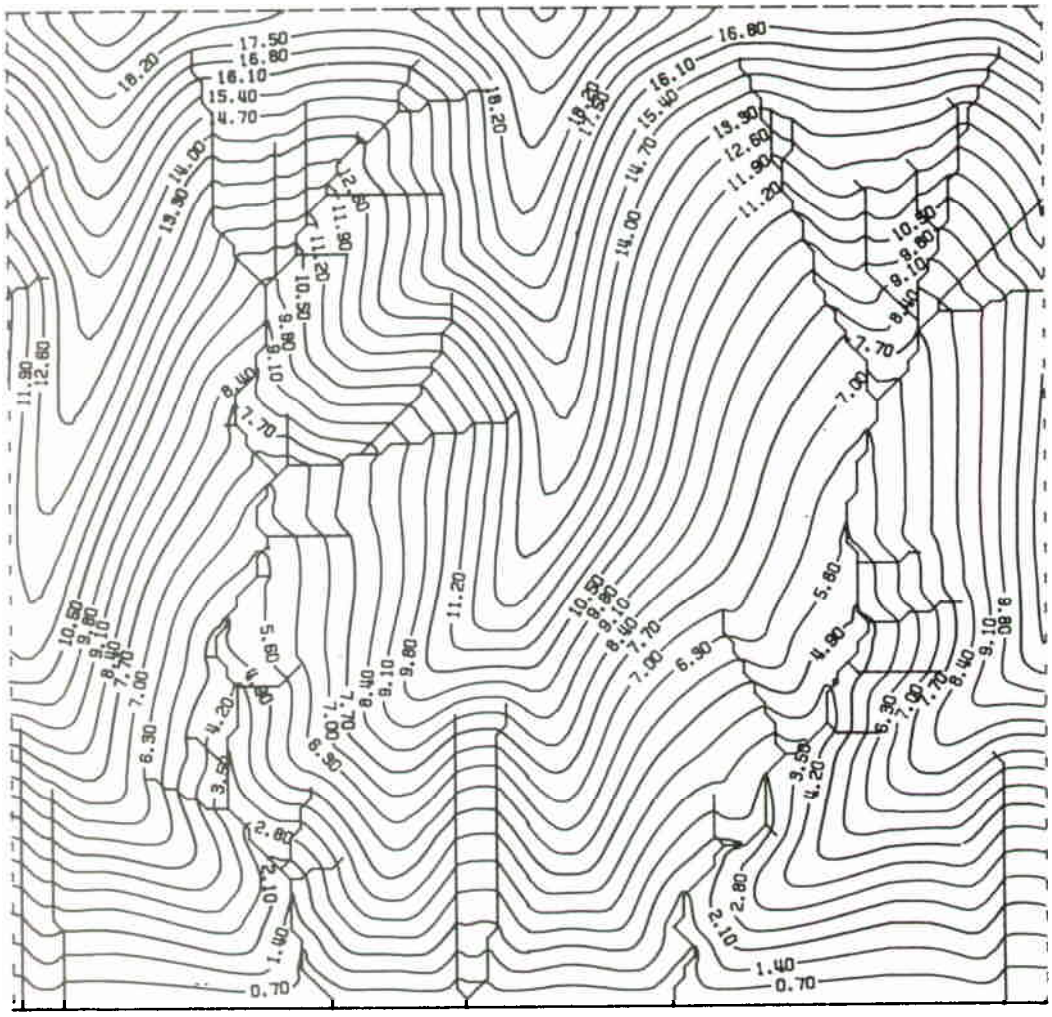

Figure 9.19 Topographic map of simulated drainage basins. Simulations are conducted on a 100 × 100 matrix. The lower boundary is assumed to be a horizontal base level which is being lowered at a constant rate. The upper boundary is a drainage divide (no water or sediment may cross that boundary), and the lateral boundary is periodic, in that water or mass leaving one boundary comes in at the other. See text for further explanation.

Initial conditions are usually a very low relief, nearly level surface with a random initial topography (including undrained depressions). The simulation is run to a nearly steady state topography (≈15 000 iterations). The simplest model assumes $\alpha = 1$, $\tau_c = 0$, $K_t = 0$, $\eta = 1$ and $\beta = 1$. This results in a superposition of regolith creep proportional to slope angle and water erosion proportional to the shear stress. For an assumed grid spacing of unity the following values give a reasonable drainage density: $K_c = K_e = 1$, $K_s = 2$, $\gamma = 0.35$, $\delta = 0.7$ with an erosion rate $E_t = 1$. This produces a dominantly concave topography with narrow rounded divides that is unlike most natural drainage basins (Fig. 9.19). In these simulations no attempt has been made to match the vertical scale or absolute gradients to a particular landscape; in other words, the vertical scale is arbitrary. We are concerned here primarily with areal variations in relative gradients and forms.

A more badlands-like topography is formed if a critical shear stress for water erosion is introduced. The topography shown in Figure 9.20 has parameter values as above except that $\tau_c = 2.5$. The divides are narrow but rounded, and the slope profiles are slightly concave. This topography is similar to that in the Mancos Shale badlands except for the concave lower slopes. A topography similar to that in the very rounded Morrison Shale badlands results if the critical shear stress is made higher and weathered shale is considered to be more easily eroded than bedrock (Fig. 9.21, with $\eta = 6$ and $\tau_c = 5.0$).

The lower slopes of high-relief badlands in all three formations (Morrison, Summerville, and Mancos) were inferred above to have gradients close

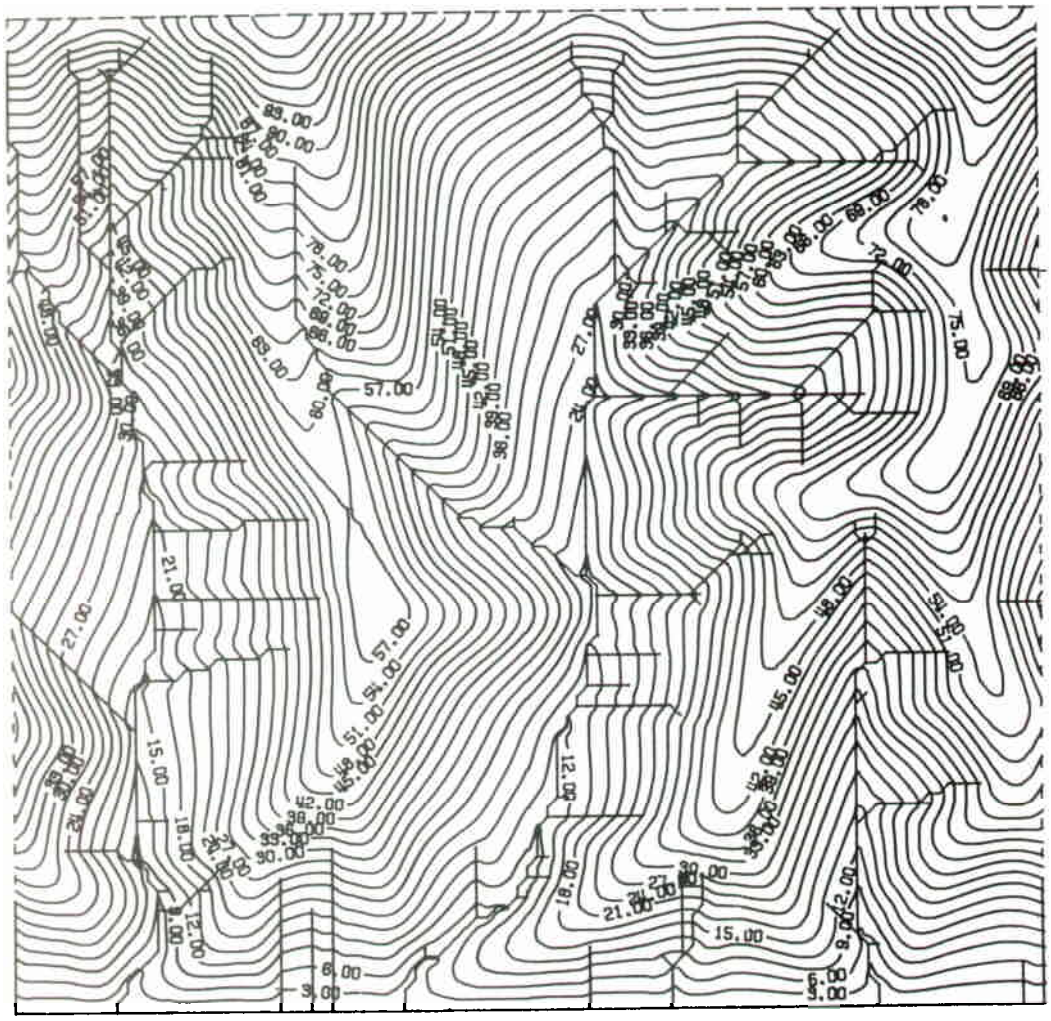

Figure 9.20 Topographic map of simulated drainage basins. Conditions are as for Figure 9.19 except that a critical threshold for fluvial erosion is assumed.

enough to the bulk stability of the weathered mantle that average mass wasting rates are enhanced relative to normal creep processes. This can be simulated in the model by giving non-zero values to K_t and ε. Figure 9.22 shows a simulation with parameters similar to Figure 9.21 except that $E_s = 0.5$, $K_t = 2.5$, and $\varepsilon = 3$. Slopes in this simulation have nearly linear profiles except for a narrow, rounded crest. This simulation has slope forms most similar to the Summerville Formation badlands of any of the simulations shown here, and is also similar to those on the Mancos Shale except for the less rounded divides on Mancos Shale.

The simulations shown here have assumed a constant rate of base level lowering, so that steady state topography eventually develops from any initial conditions. Under these conditions all parts of the landscape erode vertically at a constant rate, and the volume of regolith eroded per unit surface area per unit time V_{at} decreases with the slope angle θ:

$$V_{at} = h_t \cos\theta \qquad (9.17)$$

The simulation model at present assumes low slope gradients so that the cosine term can be approximated by unity. However, for explicit modelling of badland slopes this correction should be made. Equation 9.17 also explains the common lack of correlation between slope steepness and badland erosion rates (Schumm 1956a, Schumm and Lusby 1963, Campbell 1970, 1974, 1982); little correlation would be expected for steady state badland slopes.

The model does not directly specify the drainage density or the source locations of streams. Rather, the simulation parameters determine the transition from convex slopes to linear channels. A critical value of the convergence of slope gradient $-\nabla \cdot \mathbf{S}/\hat{S}$,

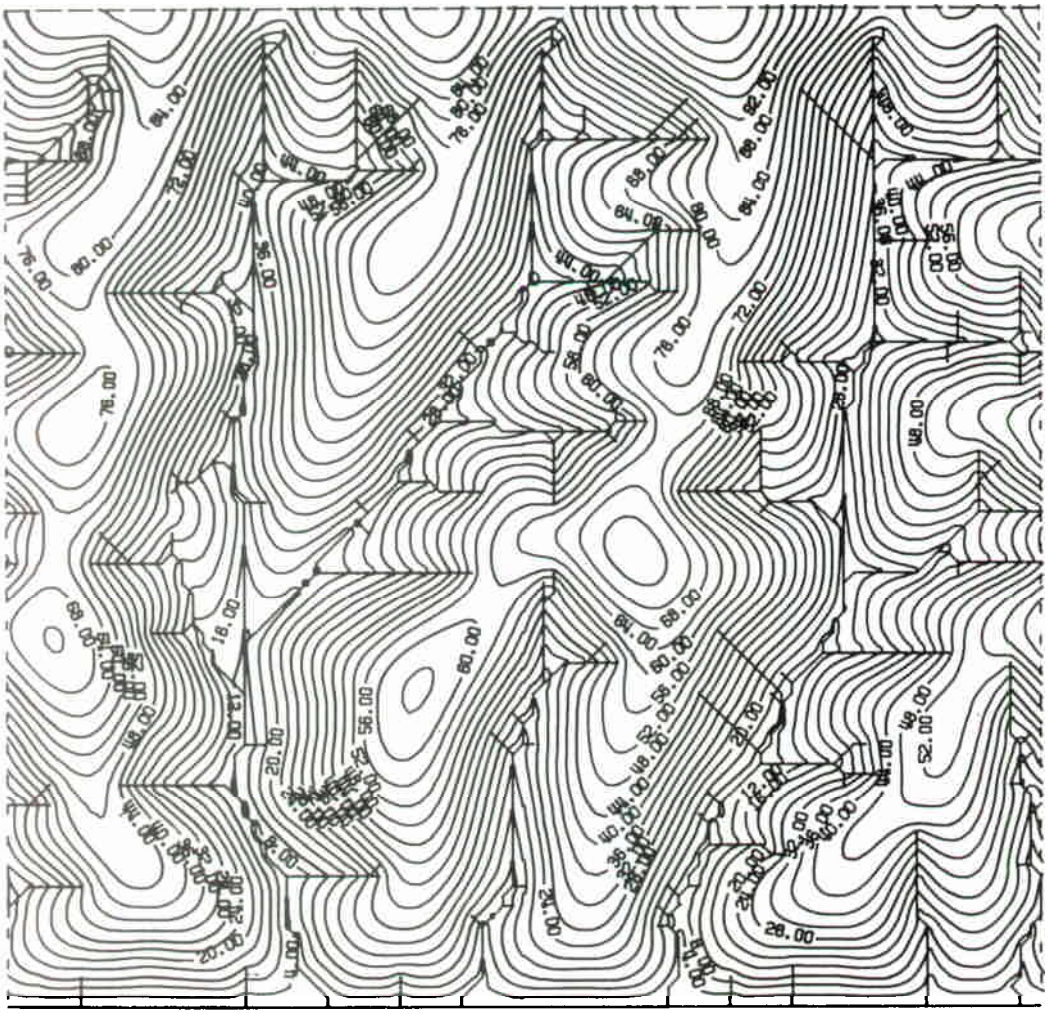

Figure 9.21 Topographic map of simulated drainage basins. Conditions are as in Figure 9.20 except that the threshold for channel erosion is higher and mass wasted regolith is assumed to be easier to fluvially erode than is bedrock.

where $\hat{S}$ is the average basin gradient, provides a reasonable definition of channel locations, giving a generally connected drainage network that corresponds closely with the usual contour crenelation method. This criterion has been used to define the drainage pattern in the illustrated basins.

Several generalities can be made about the landform development and spatial organization of process and topography in these steady state models.

(a) The model is deterministic, with randomness involved only in the development of the initial low-relief topography. The simulations show that even a small random component, either as initial or boundary conditions, is sufficient to provide the rich variation in landform texture that characterizes natural landscapes.

(b) For a constant rate of base level lowering a steady state topography is eventually developed for any arbitrary initial topography. The steady state topographies produced from different initial conditions are all different in detail but similar in general form (e.g. distributions of hillslope and channel gradients, drainage density, and slope profile characteristics).

(c) Very simple additive models of erosional processes produce landforms with spatial properties similar to natural drainage basins. This suggests that, despite the temporal and spatial complexity of processes acting in badlands, long-term erosion of badlands can be approximated through the use of reasonably simple models.

(d) Validation of simulation models of drainage basin development is hampered by very limited

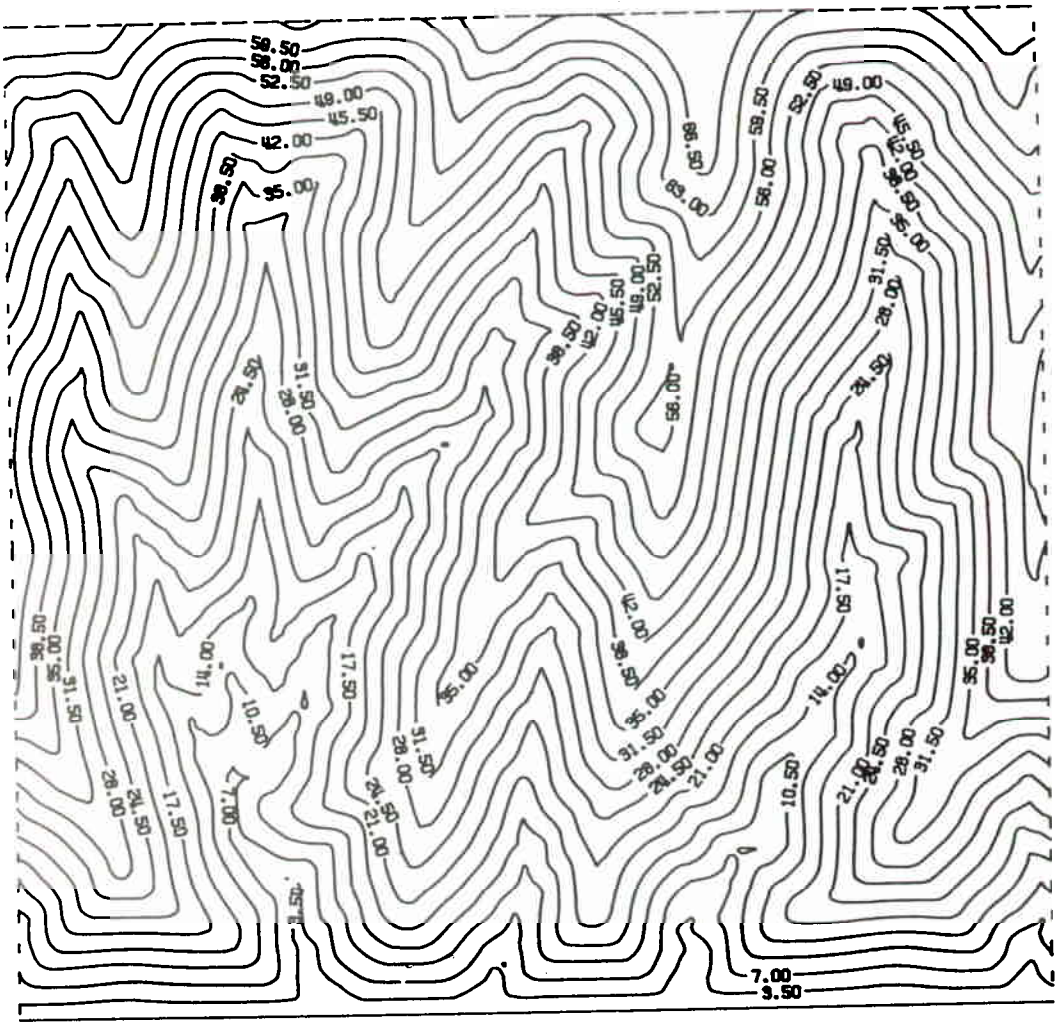

Figure 9.22 Topographic map of simulated drainage basins with a critical gradient for slope failure.

opportunity to compare predicted with observed landform evolution. Therefore, morphometric comparison of simulated and natural drainage basins is a useful technique but will require development of new means of characterizing landform scale, length, orientation, and relief properties. Possible approaches include statistical measures of hypsometry, gradients, junction angles, slope profiles, fractal properties, topology, and frequency-domain analysis.

(e) As has been noted in field measurements of badland erosion, the relative importance of water erosion increases from the divide through the lower slopes to the streams. Even where there is a critical threshold for water erosion ($\tau_c > 0$, as in Figs 9.20 and 9.21) the lower, unchannelled portions of the slopes are commonly partly eroded by water runoff.

(f) The drainage pattern exhibits strong pattern optimization in the sense used by Howard (1990), in that drainage paths from source to outlet are reasonably direct and the drainage density is nearly uniform.

The overall spatial variation in badland morphology may be an indicator of the erosional history of the area. As an obvious example, dissection of a terrace progresses inward from the terrace edge, progressing fastest along streams with the greatest drainage (Schumm 1956a). Because the model at present does not encompass alluvial washes and alluvial surfaces, it cannot be used to simulate erosional history of the Mancos Shale badlands in the Caineville area, where such surfaces are presently expanding into the badlands. However, Howard (1970) utilized a model that investigated the evolution of both bedrock

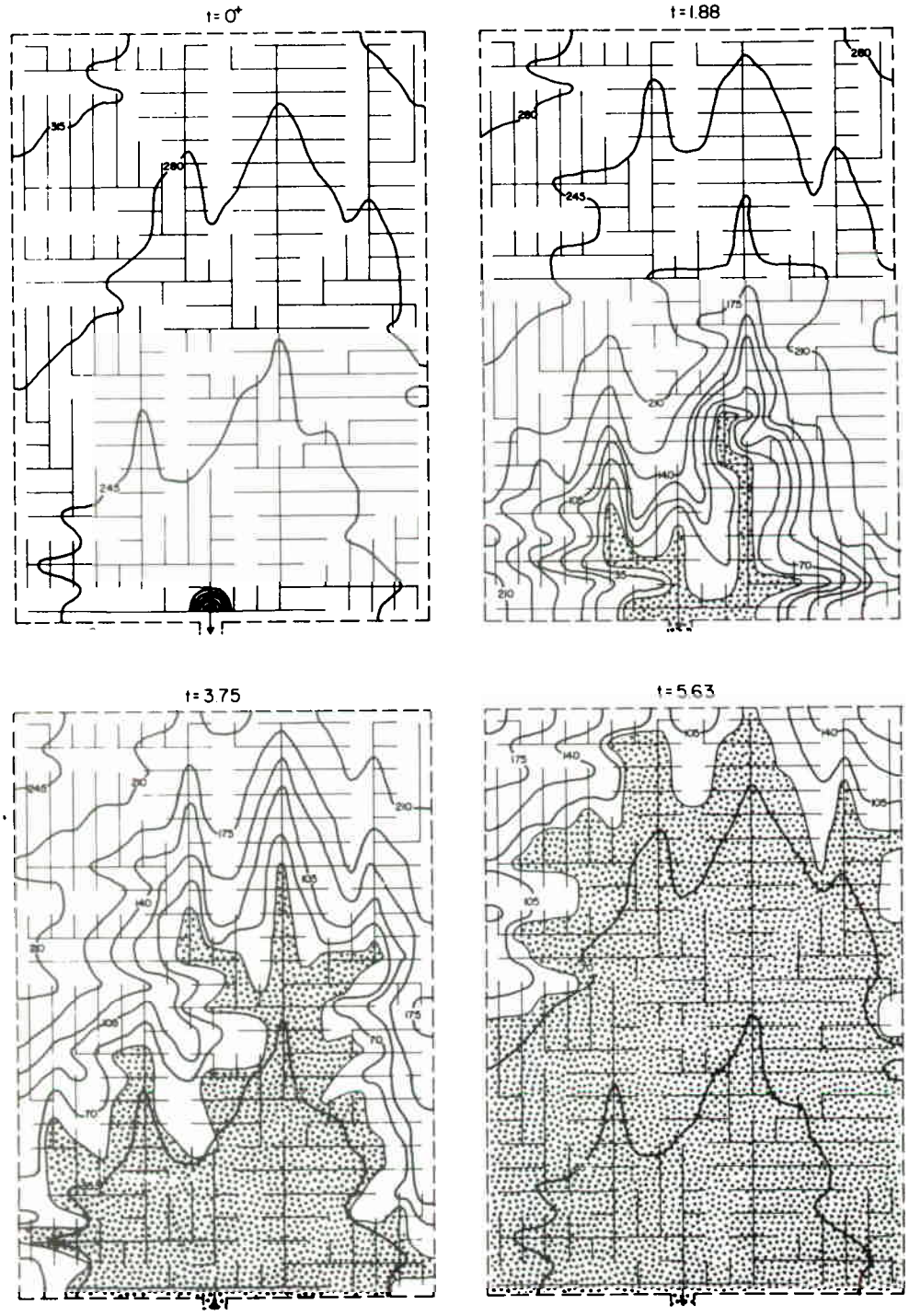

Figure 9.23 Successive stages in the dissection of an alluvial surface after an instantaneous lowering of the downstream end of the basin, followed by stability. Where erosion proceeds to the point that stream gradients reach the assumed minimum value necessary to transport sediment supplied from upstream (equation 9.13), no further erosion is permitted and an alluvial surface is formed (shaded pattern). The relative time since the beginning of the dissection is given by t.

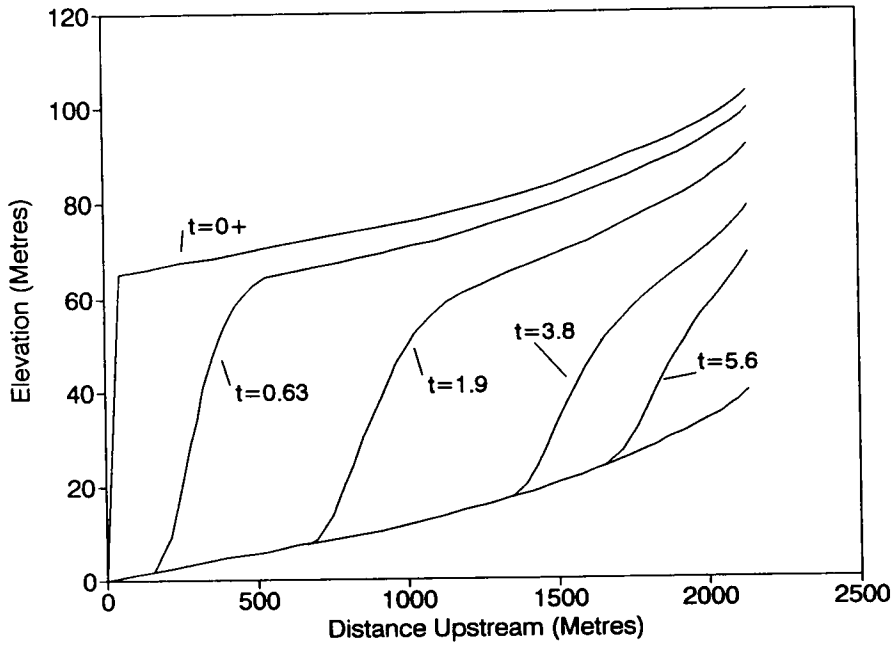

Figure 9.24 Stream profiles developed at successive stages in the dissection of the alluvial surface shown in Figure 9.23. The profile is taken along the stream heading in the upper left-hand corner of Figure 9.23.

washes (using the same approach as indicated in equations 9.7 and 9.8) and alluvial surfaces in this area. But this model does not simulate slope development and assumes a uniform drainage density. Two scenarios were investigated. In both the initial conditions are a flat, undissected alluvial surface assumed to represent the Bull Lake surface. In the first scenario it is assumed that the downstream end of the alluvial surface is instantaneously lowered but then remains stable at the lower level. This scenario represents a sudden downcutting of the Fremont River followed by stability at its present level. Figure 9.23 shows successive stages of dissection of the surface with contours on the badland washes and the extent of development of new alluvial surface graded to the lower river level; Figure 9.24 shows successive stream profles along the main stream. In the second scenario there is a uniform rate of base level lowering (Fig. 9.25), and the extent of alluvial surface depends upon the rate of lowering. In this simulation the extent of alluvial surface does not vary with time and occupies all areas greater than a critical drainage area whose value decreases with increasing downcutting rate. Howard (1970) concluded that the sudden downcutting followed by stability provides a better representation of the actual distribution of alluvial surface (Fig. 9.7), which is greater near the Fremont River and is not a simple function of contributing area.

In conclusion, the use of simulation models for addressing landform evolution in badlands (and drainage basins in general) has a bright future. The most important challenges in using such models are (a) developing appropriate process rate laws; (b) determining the boundary conditions (temporal and spatial) for the given situation; and (c) validation of the model through comparison of process rates or landform morphology between the model and the target natural landscape. Each of these issues is complicated. For example, because of the sensitivity of exact landform morphology to initial and boundary conditions, long-term simulations of landform development cannot be expected to exactly duplicate a specific natural landscape. Comparisons between simulated and natural landscape will need to be statistical; this involves judgments on what variables are most important in making such comparisons and what level of agreement is satisfactory. Similarly, it may be uncertain to what degree the process assumptions in the model are validated by successful statistical comparisons with a natural landscape; rather different mathematical models may be capable of producing similar landforms. Even if the mathematical structure of the model is validated by strong statistical correspondences, it may still be uncertain what actual processes correspond to the mathematical model (e.g. diffusive transport can be produced by regolith creep, rain-splash, or some types of runoff: Dunne and Aubrey 1986).

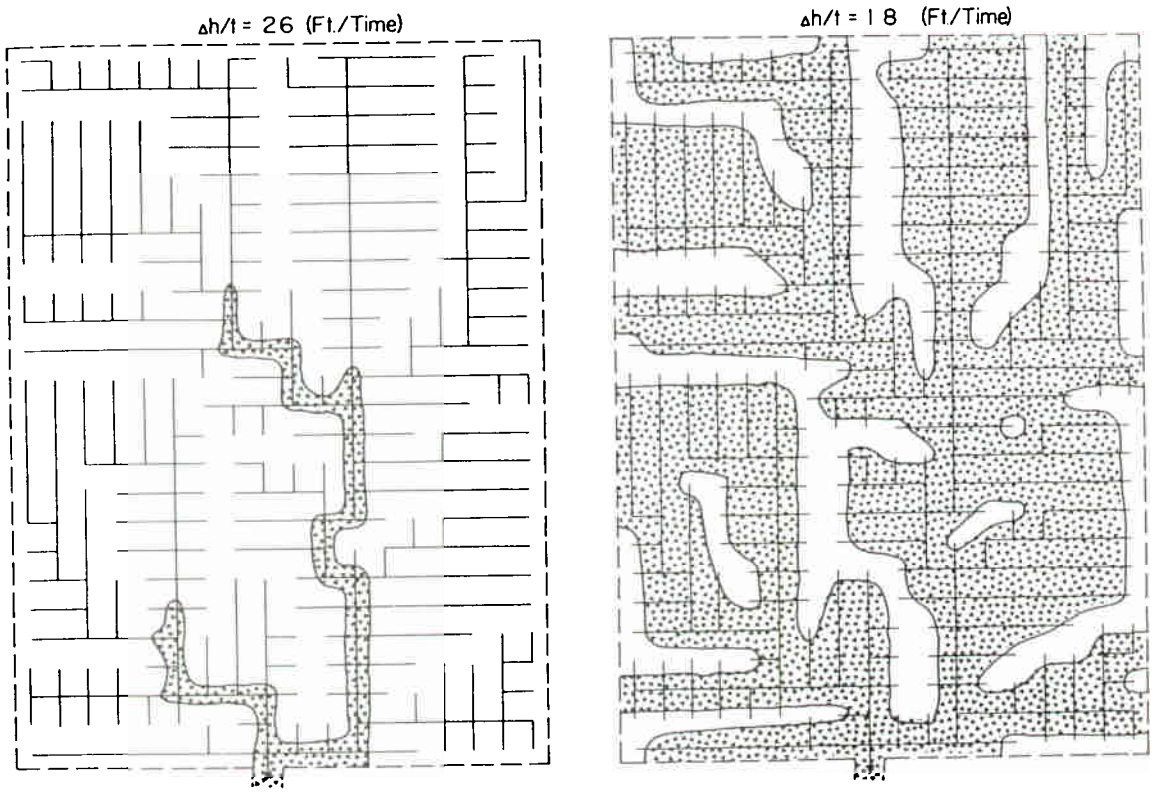

Figure 9.25 Distribution of alluvial surface (shaded) and bedrock channels (unshaded) during dissection of an alluvial surface by a constant rate of lowering of the downstream end of the basin. The vertical downcutting rate per unit time (arbitrary units) is given by $\Delta h/t$. For a value of $\Delta h/t$ less than about 13 the entire area remains as alluvial surface, while for values greater than 53 no alluvial surface remains.

CONCLUSIONS

Despite a long history of badland studies, many uncertainties remain concerning badland processes and landform development. Further understanding of badlands will require studies conducted at a range of temporal and spatial scales. There is a need for observational and experimental studies of hydraulic processes, regolith weathering, and erosion at the scale of small plots to small drainage basins at the timescale of individual precipitation events to extend the pioneering work of Bryan *et al.* (1978, 1984), Hodges (1982), and Yair *et al.* (1980) to the full range of bedrock types, relief, and climates supporting badlands. At an intermediate spatio-temporal scale there is a paucity of coordinated measurement of total, rainsplash, runoff, and mass wasting erosion and regolith development on the scale of small drainage basins and over a period of several years. The relative roles of these processes and their spatial distribution within badland drainage basins is still largely unconstrained. At the largest scale is the opportunity to decipher regional landform evolution in badlands and to relate variations in badland form to erosional history. Finally, comparative study of badlands of different rock type, climate, or erosional histories can be productive at any of these scales.

Badlands offer a unique opportunity for development and testing of quantitative landform models because we not only have the landform morphology to compare with theoretical models but processes are rapid enough that rates of landform change can be measured with reasonable accuracy over periods of just a few years.

REFERENCES

Ahnert, F. 1976. Brief description of a comprehensive three-dimensional process-response model of landform development. *Zeitschrift für Geomorphologie Supplement Band* **25**, 29–49.

Ahnert, F. 1977. Some comments on the quantitative formulation of geomorphological processes in a theoretical model. *Earth Surface Processes* **2**, 191–202.

Ahnert, F. 1987a. Approaches to dynamic equilibrium in theoretical simulations of slope development. *Earth Surface Processes and Landforms* **12**, 3–15.

Ahnert, F. 1987b. Process-response models of denudation at different spatial scales. *Catena Supplement* **10**, 31–50.

Ahnert, F. 1988. Modelling landform change. In *Modelling Geomorphological Processes*, M.G. Anderson (ed.), 375–400. Chichester: Wiley.

Akky, M.R. and C.K. Shen 1973. Erodibility of a cement-stabilized sandy soil. In *Soil erosion: causes and mechanisms*. U.S. Highway Research Board Special Report 135, 30–41.

Ariathurai, R. and K. Arulandan 1986. Erosion rates of cohesive soils. *Journal of the Hydraulics Division, Proceedings of the American Society of Civil Engineers* **104**, 279–98.

Bowyer-Bower, T.A.S. & R.B. Bryan 1986. Rill initiation: concepts and evaluation on badland slopes. *Zeitschrift für Geomorphologie Supplement Band* **59**, 161–75.

Bradley, W.H. 1940. Pediments and pedestals in miniature. *Journal of Geomorphology* **3**, 244–54.

Bryan, R.B. 1987. Processes and significance of rill development. *Catena Supplement* **8**, 1–15

Bryan, R.B., I.A. Campbell and A. Yair 1987. Postglacial geomorphic development of the Dinosaur Provincial Park badlands, Alberta. *Canadian Journal of Earth Sciences* **24**, 135–46.

Bryan, R.B., A.C. Imeson and I.A. Campbell 1984. Solute release and sediment entrainment on microcatchments in the Dinosaur Park badlands, Alberta, Canada. *Journal of Hydrology* **71**, 79–106.

Bryan, R. and A. Yair, 1982a. Perspectives on studies of badland geomorphology. In *Badland geomorphology and piping*. R. Bryan and A. Yair (eds), 1–13. Norwich: Geo Books.

Bryan, R. and A. Yair (eds) 1982b. *Badland geomorphology and piping*. Norwich: Geo Books.

Bryan, R.B., A. Yair and W.K. Hodges 1978. Factors controlling the initiation of runoff and piping in Dinosaur Provincial Park badlands, Alberta, Canada. *Zeitschrift für Geomorphologie Supplement Band* **34**, 48–62.

Campbell, I.A. 1970. Erosion rates in the Steveville badlands, Alberta. *The Canadian Geographer* **14**, 202–16.

Campbell, I.A. 1974. Measurements of erosion on badlands surfaces. *Zeitschrift für Geomorphologie Supplement Band* **21**, 122–37.

Campbell, I.A. 1982. Surface morphology and rates of change during a ten-year period in the Alberta badlands. In *Badland geomorphology and piping*, R. Bryan and A. Yair (eds), 221–36. Norwich: Geo Books.

Campbell, I.A. 1989. Badlands and badland gullies. In *Arid zone geomorphology*, D.S.G. Thomas (ed.), 159–93. New York: Halstead Press.

Campbell, I.A. and J.L. Honsaker 1982. Variability in badlands erosion; problems of scale and threshold identification. In *Space and time in geomorphology*, C.E. Thorn, (ed.), 59–79. London: George Allen & Unwin.

Carman, M.F., Jr 1958. Formation of badland topography. *Bulletin of the Geological Society of America* **69**, 789–90.

Carson, M.A. 1969. Models of hillslope development under mass failure. *Geographical Analysis* **1**, 76–100.

Carson, M.A. 1971. An application of the concept of threshold slopes to the Laramie Mountains, Wyoming. *Institute of British Geographers Special Publication* 3, 31–47.

Carson, M.A. and M.J. Kirkby 1972. *Hillslope form and process*. Cambridge: Cambridge University Press.

Carson, M.A. and D.J. Petley 1970. The existence of threshold slopes in the denudation of the landscape. *Transactions of the Institute of British Geographers* **49**, 71–95.

Chisci, G., M. Sfalanga and D. Torri 1985. An experimental model for evaluating soil erosion on a single-rainstorm basis. In *Soil erosion and conservation*, S.A. Swaify, W.C. Moldenhauer and A. Lo (eds), 558–65. Ankeny, IA: Soil Conservation Society of America.

Churchill, R.R. 1981. Aspect-related differences in badlands slope morphology. *Annals of the Association of American Geographers* **71**, 374–88.

Culling, W.E.H. 1963. Soil creep and the development of hillside slopes. *Journal of Geology* **71**, 127–61.

Davis, W.M. 1892. The convex profile of bad-land divides. *Science* **20**, 245.

Dunne, T. and B.F. Aubrey 1986. Evaluation of Horton's theory of sheetwash and rill erosion on the basis of field experiments. In *Hillslope processes*, A.D. Abrahams (ed.), 31–53. Boston: Allen & Unwin.

Emmett, W.W. 1970. The hydraulics of overland flow on hillslopes. *U.S. Geological Survey Professional Paper* 662-A.

Engelen, G.B. 1973. Runoff processes and slope development in Badlands National Monument, South Dakota. *Journal of Hydrology* **18**, 55–79.

Everaert, W. 1991. Empirical relations for the sediment transport capacity of interrill flow. *Earth Surface Processes and Landforms* **16**, 513–32.

Finlayson, B.L., J. Gerits and B. van Wesemael 1987. Crusted microtopography on badland slopes in southeast Spain. *Catena* **14**, 131–44.

Foster, G.R. 1982. Modeling the erosion process. In *Hydrologic modeling of small watersheds*, C.T. Hahn, H.P. Johnson and D.L. Brakensiek (eds), 297–382. St Joseph, MI: American Society of Agricultural Engineers.

Foster, G.R. 1990. Process-based modelling of soil erosion by water on agricultural land. In *Soil erosion on agricultural land*, J. Boardman, I.D.L. Foster and J.A. Dearing (eds), 429–45. Chichester: Wiley.

Foster, G.R. and L.J. Lane 1983. Erosion by concentrated flow in farm fields. In *Proceedings of the D.B. Simons symposium on erosion and sedimentation, 9.65–9.82*. Fort Collins, CO: Colorado State University.

Foster, G.R. and L.D. Meyer 1972. A closed-form soil erosion equation for upland areas. In *Sedimentation (Einstein)*, H.W. Shen (ed.), 12.1–12.19. Fort Collins, CO: Colorado State University.

Gerits, J., A.C. Imeson, J.M. Verstraten and R.B. Bryan 1987. Rill development and badland regolith properties. *Catena Supplement* **8**, 141–60.

Gilbert, G.K. 1880. *Report on the geology of the Henry Mountains*. Washington: U.S. Geographical and Geological Survey of the Rocky Mountain Region.

Gilbert, G.K. 1909. The convexity of hilltops. *Journal of Geology* **17**, 344–51.

Gilley, J.E., D.A. Woolhiser and D.B. McWhorter 1985. Interrill soil erosion – part I: development of model equations. *Transactions of the American Society of Agricultural Engineers* **28**, 147–53, 159.

Govers, G. 1985. Selectivity and transport capacity of thin flows in relation to rill erosion. *Catena* **12**, 35–49.

Govers, G. and G. Rauws 1986. Transporting capacity of overland flow on plane and on irregular beds. *Earth Surface Processes and Landforms* **11**, 515–24.

Harvey, A. 1982. The role of piping in the development of badlands and gully systems in south-east Spain. In

Badland geomorphology and piping, R. Bryan and A. Yair (eds), 317–35. Norwich: Geo Books.

Hirano, M. 1975. Simulation of developmental process of interfluvial slopes with reference to graded form. *Journal of Geology* **83**, 113–23.

Hodges, W.K. 1982. Hydraulic characteristics of a badland pseudo-pediment slope system during simulated rainstorm experiments. In *Badland geomorphology and piping*, R. Bryan and A. Yair (eds), 127–51. Norwich: Geo Books.

Hodges, W.K. and R.B. Bryan 1982. The influence of material behavior on runoff initiation in the Dinosaur Badlands, Canada. In *Badland geomorphology and piping*, R. Bryan and A. Yair (eds), 13–46. Norwich: Geo Books.

Howard, A.D. 1970. A study of process and history in desert landforms near the Henry Mountains, Utah. Unpublished Ph.D. dissertation. Baltimore: Johns Hopkins University.

Howard, A.D. 1980. Thresholds in river regime. In *Thresholds in geomorphology*, D.R. Coates and J.D. Vitek (eds), 227–58. London: George Allen & Unwin.

Howard, A.D.. 1982. Equilibrium and time scales in geomorphology: application to sand-bed alluvial channels. *Earth Surface Processes and Landforms* **7**, 303–25.

Howard, A.D. 1986. Quaternary landform evolution of the Dirty Devil River system, Utah. *Geological Society of America Abstracts with Program*, 641.

Howard, A.D. 1990. Theoretical model of optimal drainage networks. *Water Resources Research* **26**, 2107–17.

Howard, A.D. 1992. Issues in drainage basin modelling: drainage density, drainage pattern, randomness, and validation. *In preparation*.

Howard, A.D. and G. Kerby 1983. Channel changes in badlands. *Bulletin of the Geological Society of America* **94**, 739–52.

Hunt, C.B. 1953. Geology and geography of the Henry Mountains region. *U.S. Geological Survey Professional Paper* 228.

Imeson, A.C. and J.M. Verstraten 1985. The erodibility of highly calcareous soil material from southern Spain. *Catena* **12**, 291–306.

Imeson, A.C. and J.M. Verstraten 1988. Rills on badland slopes: a physico-chemically controlled phenomenon. *Catena Supplement* **12**, 139–50.

Imeson, A.C., F.J.P.M. Kwaad and J.M. Verstraten 1982. The relationship of soil physical and chemical properties to the development of badlands in Morocco. In *Badland geomorphology and piping*, R. Bryan and A. Yair (eds), 47–69. Norwich: Geo Books.

Jones, J.A.A. 1990. Piping effects in drylands. *Geological Society of America Special Paper* 252, 111–38.

Julian, P.Y. and D.B. Simons 1985. Sediment transport capacity of overland flow. *Transactions of the American Society of Agricultural Engineers* **28**, 755–62.

Karcz, I. and D. Kersey, 1980. Experimental study of free-surface flow instability and bedforms in shallow flows. *Sedimentary Geology* **27**, 263–300.

Kinnell, P.I.A. 1990 Modelling erosion by rain-impacted flow. *Catena Supplement* **17**, 55–66.

Kinnell, P.I.A. 1991. The effect of flow depth on sediment transport induced by raindrops impacting shallow flows. *Transactions of the American Society of Agricultural Engineers* **34**, 161–8.

Kirkby, M.J. 1971. Hillslope process-response models based on the continuity equation. *Institute of British Geographers Special Publication* 3, 15–30.

Kirkby, M.J. 1976a. Soil development models as a component of slope models. *Earth Surface Processes* **2**, 203–30.

Kirkby, M.J. 1976b. Deterministic continuous slope models. *Zeitschrift für Geomorphology Supplement Band* **25**, 1–19.

Kirkby, M.J. 1980. Modelling water erosion processes. In *Soil erosion*, M.J. Kirkby and R.P.C. Morgan (eds), 183–216. Chichester: Wiley.

Kirkby, M.J. 1984. Modelling cliff development in south Wales. Savigear re-viewed. *Zeitschrift für Geomorphologie* **28**, 405–26.

Kirkby, M.J. 1985a. The basis for soil profile modelling in a geomorphic context. *Journal of Soil Science* **36**, 97–122.

Kirkby, M.J. 1985b. A model for the evolution of regolith-mantled slopes. In *Models in geomorphology*, M.J. Woldenberg (ed.), 213–37. Boston: Allen & Unwin.

Kirkby, M.J. 1986. A two-dimensional simulation model for slope and stream evolution. In *Hillslope processes*, A.D. Abrahams (ed.), 203–22. Boston: Allen & Unwin.

Kirkby, M.J. 1990. A one-dimensional model for rill inter-rill interactions. *Catena Supplement* **17**, 133–46.

Komura, S. 1976. Hydraulics of slope erosion by overland flow. *Journal of the Hydraulics Division, Proceedings of the American Society of Civil Engineers* **102**, 1573–86.

Kuijper, C., J.M. Cornelisse and J.C. Winterwerp 1989. Research on erosive properties of cohesive sediments. *Journal of Geophysical Research* **94**, 14341–50.

Lambe, T.W. and R.V. Whitman 1969. *Soil mechanics*. New York: Wiley.

Lane, L.J., E.D. Shirley and V.P. Singh 1988. Modelling erosion on hillslopes. In *Modelling geomorphological systems*, M.G. Anderson (ed.), 287–308. Chichester: Wiley.

Laronne, J.B. 1981. Dissolution kinetics of Mancos Shale – associated alluvium. *Earth Surface Processes and Landforms* **6**, 541–52.

Laronne, J.B. 1982. Sediment and solute yield from Mancos Shale hillslopes, Colorado and Utah. In *Badland geomorphology and piping*, R. Bryan and A. Yair (eds), 181–92. Norwich: Geo Books.

Mackin, J.H. 1948. Concept of the graded river. *Bulletin of the Geological Society of America* **59**, 463–512.

Meyer, L.D. 1986. Erosion processes and sediment properties for agricultural cropland. In *Hillslope processes*, A.D. Abrahams (ed.), 55–76. Boston: Allen & Unwin.

Meyer, L.D. and E.J. Monke 1965. Mechanics of soil erosion by rainfall and overland flow. *Transactions of the American Society of Agricultural Engineers* **8**, 572–7, 580.

Moseley, M.P. 1973. Rainsplash and the convexity of badland divides. *Zeitschrift für Geomorphologie Supplement Band* **18**, 10–25.

Moss, A.J. and P.H. Walker 1978. Particle transport by continental water flow in relation to erosion, deposition, soils and human activities. *Sedimentary Geology* **20**, 81–139.

Moss, A.J., P.H. Walker and J. Hutka 1979. Raindrop-stimulated transportation in shallow water flows: an experimental study. *Sedimentary Geology* **22**, 165–84.

Moss, A.J., P. Green and J. Hutka 1982. Small channels: their experimental formation, nature and significance. *Earth Surface Processes and Landforms* **7**, 401–16.

Parchure, T.M. and A.J. Mehta 1985. Erosion of soft cohesive sediment deposits. *Journal of the Hydaulics Divi-*

sion, Proceedings of the American Society of Civil Engineers **111**, 1308–26.

Parker, G.G., Sr, C.G. Higgins and W.W. Wood 1990. Piping and pseudokarst in drylands. *Geological Society of America Special Paper* **252**, 77–110.

Parthenaides, E. 1965. Erosion and deposition of cohesive soils. *Journal of the Hydraulics Division, Proceedings of the American Society of Civil Engineers* **91**, 105–39.

Parthenaides, E. and R.R. Paaswell 1970. Erodibility of channels with cohesive banks. *Journal of the Hydraulics Division, Proceedings of the American Society of Civil Engineers* **96**, 755–71.

Rauws, G. 1987. The initiation of rills on plane beds of non-cohesive sediments. *Catena Supplement* **8**, 107–18.

Rauws, G. and G. Govers 1988. Hydraulic and soil mechanical aspects of rill generation on agricultural soils. *Journal of Soil Science* **39**, 111–24.

Savat, J. 1976. Discharge velocities and total erosion of a calcareous loess: a comparison between pluvial and terminal runoff. *Revue Geomorphologie Dynamique* **24**, 113–22.

Savat, J. 1980. Resistance to flow in rough supercritical sheetflow. *Earth Surface Processes* **5**, 103–22.

Savat, J. 1982. Common and uncommon selectivity in the process of fluid transportation: field observations and laboratory experiments on bare surfaces. *Catena Supplement* **1**, 139–60.

Savat, J. and J. De Ploey 1982. Sheetwash and rill development by surface flow. In *Badland geomorphology and piping*, R. Bryan and A. Yair (eds), 113–25. Norwich: Geo Books.

Schumm, S.A. 1956a. Evolution of drainage systems and slopes in badlands at Perth Amboy, New Jersey. *Bulletin of the Geological Society of America* **67**, 597–646.

Schumm, S.A. 1956b. The role of creep and rainwash on the retreat of badland slopes. *American Journal of Science* **254**, 693–706.

Schumm, S.A. 1962. Erosion on miniature pediments in Badlands National Monument, South Dakota. *Bulletin of the Geological Society of America* **73**, 719–24.

Schumm, S.A. 1963. Rates of surficial rock creep on hillslopes in western Colorado. *Science* **155**, 560–1.

Schumm, S.A. 1964. Seasonal variations of erosion rates and processes on hillslopes in western Colorado. *Zeitschrift für Geomorphologie Supplement Band* **5**, 215–38.

Schumm, S.A. and G.C. Lusby 1963. Seasonal variation of infiltration capacity and runoff on hillslopes in western Colorado. *Journal of Geophysical Research* **68**, 3655–66.

Seidl, M.A. and W.E. Dietrich 1991. Bedrock channel incision: an examination of Playfair's Law. *Geological Society of America Abstracts with Program*, A240.

Slaymaker, O. 1982. The occurrence of piping and gullying in the Penticton glacio-lacustrine silts, Okanagan Valley, B.C. In *Badland geomorphology and piping*, R. Bryan and A. Yair (eds), 305–16. Norwich: Geo Books.

Smith, K.G. 1958. Erosional processes and landforms in Badlands National Monument, South Dakota. *Bulletin of the Geological Society of America* **69**, 975–1008.

Smith, T.R. and F.P. Bretherton 1972. Stability and the conservation of mass in drainage basin evolution. *Water Resources Research* **8**, 1506–29.

Torri, D., M. Sfalanga and G. Chisci 1987. Threshold conditions for incipient rilling. *Catena Supplement* **8**, 97–115.

Wells, S.G. and A.A. Gutierrez 1982. Quaternary evolution of badlands in the southeastern Colorado Plateau, U.S.A. In *Badland geomorphology and piping*, R. Bryan and A. Yair (eds), 239–57. Norwich: Geo Books.

Willgoose, G., R.L. Bras and I. Rodriguez-Iturbe 1991a. A coupled channel network growth and hillslope evolution model, 1. theory. *Water Resources Research* **27**, 1671–84.

Willgoose, G., R.L. Bras and I. Rodriguez-Iturbe 1991b. A coupled channel network growth and hillslope evolution model, 2, nondimensionalization and applications. *Water Resources Research* **27**, 1685–96.

Willgoose, G., R.L. Bras and I. Rodriguez-Iturbe 1991c. Results from a new model of river basin evolution. *Earth Surface Processes and Landforms* **16**, 237–54.

Yair, A., H. Lavee, R.B. Bryan and E. Adar 1980. Runoff and erosion processes and rates in the Zion Valley badlands, northern Negev, Israel. *Earth Surface Processes* **5**, 205–25.